

SYNTHESIS OF
ICETEXANE NATURAL PRODUCT SCAFFOLDS

by

Alisha Wang

A dissertation submitted to the Faculty of the University of Delaware in partial fulfillment of the requirements for the degree of Honors Bachelor of Science in Chemistry with Distinction

Spring 2024


© 2024 Alisha Wang

All Rights Reserved

**SYNTHESIS OF
ICETEXANE NATURAL PRODUCT SCAFFOLDS**

by

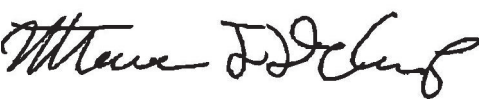
Alisha Wang

Approved: 

William Chain, Ph.D.
Professor in charge of thesis on behalf of the Advisory Committee

Approved: 

Marco Messina, Ph.D.
Committee member from the Department of Chemistry and Bioch

Approved: 

Matthew Decamp, Ph.D.
Committee member from the Board of Senior Thesis Readers

Approved: _____
Dana Veron, Ph.D.
Chair of the University Committee on Student and Faculty Honor

ACKNOWLEDGMENTS

First of all, I would like to express my gratitude toward Professor William J. Chain not only for the opportunity to conduct research in his laboratory but also his guidance, advising, and encouragement. I have been able to grow so much in the past three years due to his mentorship and the opportunities to teach, intern, and conduct research. I now confidently anticipate the following years as a graduate student at B.J.'s alma mater.

I would like to thank my committee members Professor Marco Messina and Professor Matthew Decamp for their input and guidance.

In a throwback to the summer of 2022, I would like to give a big shout-out to the OGs, Alexandre Ziegelmeier and Liam O'Grady, for being the best labmates I could ask for. I accidentally became Alex's mentee two years ago and I am forever grateful for his role in making my undergraduate research career as smooth as it has been. I will sincerely miss Alex and Liam both as mentors and friends, and hope to one day be able to proudly stand next to them on the same level.

I would like to thank all my graduate colleagues, Leah White, Nicole Kretekos, Shelby Cooper, Kyle Hess, Tyler Swanson, Dr. Eli Hudson, Dr. Ali Amiri Naeini, and David Detloff. I have felt an increasing sense of camaraderie and belonging over the years. I am grateful to you all for treating me as a peer and giving me a home. Leah, I unfortunately cannot stay and be your mentee </3. Nicole and Shelby, I appreciated your support and companionship during trying times. I would also like to personally thank Kyle for kicking me out of my hood twice. I will greatly miss all of you for creating such a welcoming and entertaining environment.

I would like to thank all my undergraduate colleagues, Matthew Kaganovich, Finn Davis, Jasmine Bioteau, Annabella Pizzurro, and Asher Chamuel. Matt was my first mentor as a fifth-

year undergraduate student also conducting his own senior thesis. As hectic as it was, I appreciate Matt taking the time for my tutelage and life conversations. I wish all my peers luck in their future endeavors.

I would like to thank my parents, Enju and Guozhi Wang, and my brother, Andreas. I cannot even begin to thank them for the support they both have and continue to give me. Their encouragement allows me to strive for their level of greatness.

I would like to thank my boyfriend, Kern Freesland. I have been able to build a healthier and happier life with his support and encouragement.

I would like to thank my friends both at home and at the University of Delaware. They were there for me whenever I needed them. Without their support and encouragement, I would not be where I am today.

TABLE OF CONTENTS

List of Figures.....	vi
Abstract.....	vii
Chapter 1. Icetexanes.....	1
1.1 Introduction.....	1
1.2 Classification.....	3
1.3 Biosynthetic Pathway.....	6
1.4 Early Synthetic Milestones.....	8
Chapter 2. Premnalatifolin A & Synthesis of Icetexane Analog Intermediates.....	12
2.1 Introduction to Premnalatifolin A.....	12
2.2 Prior Synthesis Studies.....	14
2.3 Synthetic Efforts towards the Southern Monomer of Premnalatifolin A.....	19
2.4 Synthetic Efforts towards the Northern Monomer of Premnalatifolin A.....	26
Chapter 3. Analog Synthesis Routes and Experimentation.....	30
3.1 Background and Necessity.....	30
3.2 Synthesis of Analog 3.9	31
3.3 Synthesis of Analogues 3.10 and 3.11	34
3.4 Summary.....	35
References.....	37
Experimental Procedures.....	42
Appendix.....	64
A. Catalog of Spectra.....	64

List of Figures

Figure 1.1 First discovered icetexone.....	2
Figure 1.2 Some icetexane natural products.....	3
Figure 1.3 Icetexane classification.....	4
Figure 1.4 Parents of icetexane classes.....	5
Figure 1.5 Comparison of the icetexane and abietane frameworks.....	6
Figure 1.6 First discovered synthetic link between abietanes and icetexanes.....	7
Figure 1.7 Biosynthetic pathway from abietanes to icetexanes.....	8
Figure 1.8 Synthetic route to pisiferin 1.15	9
Figure 1.9 Synthetic route to komaroviquinone 1.5	11
Figure 2.1 Structures of icetexanes isolated from <i>Premna latifolia</i>	13
Figure 2.2 Structure of doxorubicin.....	14
Figure 2.3 Synthetic route to silylenol ether 2.7 and 2.9	14
Figure 2.4 Synthetic route of benzyl chloride 2.13	15
Figure 2.5 Unsuccessful alkylation via the OQM methodology.....	16
Figure 2.6 Synthetic routes to icetexanes 2.21 , 2.22 , 2.25 and 2.26	17
Figure 2.7 Structural comparison of targeted icetexanes 2.22 and 2.27	18
Figure 2.8 Synthetic route to 2.30	18
Figure 2.9 Synthetic route to icetexane 2.27	19
Figure 2.10 Synthetic route to allylbenzene 2.41	21
Figure 2.11 Synthetic route to the righthand side of the southern monomer, 2.46	22
Figure 2.12 Synthetic route to icetexane 2.49	23
Figure 2.13 Synthetic route to icetexane 2.53	24

Figure 2.14 Optimization of the route to 2.57	25
Figure 2.15 Optimization of alkylation conditions.....	26
Figure 2.16 Proposed synthetic route to the northern monomer of Premnalatifolin A, 2.3.....	27
Figure 2.17 Synthetic route to icetexane 2.67	27
Figure 2.18 Synthetic route to icetexane 2.68	28
Figure 2.19 Synthetic route to icetexane 2.71	29
Figure 3.1 Functional groups of interest on icetexanes.....	30
Figure 3.2 Previously synthesized icetexane analogues.....	31
Figure 3.3 This work's targeted icetexane analogues.....	31
Figure 3.4 Synthetic route to the right-hand side 3.17 of analog 3.9	33
Figure 3.5 Synthetic route to analog 3.9	34
Figure 3.6 Synthetic route to analog 3.10	35

Abstract

Icetexanes are a family of natural products with a wide array of biological activities, making them desirable targets for synthetic chemists over the past decade. Chapter 1 outlines the structure and different types of icetexanes—from the first isolated icetexane to the classification system that arose from the numerous icetexanes that have since been discovered. Along with the biosynthetic pathway, chapter 1 takes a closer look at early synthetic developments towards the core structure of icetexanes.

Chapter 2 outlines the structure and biological activity of the icetexane premnalatifolin A. Chapter 2 then delves into the synthetic efforts towards premnalatifolin A conducted by Mr. Daniel J. Moon and Dr. Mohammad Al-Amin in the Chain Laboratory. Inspired by Moon and Al-Amin's works, Dr. Ali N. Amiri and Mr. Alexandre Ziegelmeier have made large strides towards the completion of both the northern and southern monomers of Premnalatifolin A.

Chapter 3 introduces the necessity for a large array of icetexane analogues. Taking inspiration from my predecessors, my efforts towards the synthesis of three conventional unnatural icetexane analogues are detailed in chapter 3.

CHAPTER 1

Icetexanes

1.1 Introduction

Medicinal plants have been used as homeopathic and natural remedies for various ailments throughout history. Although modern medicine and drug discovery have made huge progress, homeopathic remedies are still prevalent and can be purchased over-the-counter (OTC) in pharmacies. For example, a homeopathic cold medicine marketed as ColdCalm® contains low dosages of several natural products, which are constituents of the extracts of various terrestrial plants such as *Atropa belladonna* (deadly nightshade) and *Allium cepa* (common onion). The use of natural remedies in Chinese traditional medicine is still common in modern Chinese culture. One important group of herbs is thought to purge the body of interior heat and thus are considered antipyretic.¹ Such natural remedies have the potential to treat inflammatory diseases and microbial infections. A flowering plant like *Calendula officinalis* (English marigold) has been used in traditional medicine to treat wounds, ulcers, scars, frostbite, and more.² Even children's books like the *Warrior Cats* series by Erin Hunter make references to natural remedies like marigold being used to prevent infection.

Today, many drugs are developed from the natural products found in plants and have been shown to be effective against various diseases. As of this writing, approximately 25% of FDA approved drugs are derived from natural products that originate from plants.³ As such, it is often necessary and relevant to probe these various natural products for the full extent of their efficacy and utilize chemical synthesis to generate large scale quantities of these natural products.

One family of medicinally active natural products isolated from plants are icetexanes.⁴ Icetexanes are a class of natural products that contain a 6-7-6 tricyclic framework and are often isolated from plant species that also produce abietane natural products, containing a 6-6-6 tricyclic framework. The first icetexane natural product, icetexone **1.1**, was isolated alongside abietane natural product, conacytone **1.2**, in 1976 from the *Salvia Ballotaeflora* by Watson and coworkers.⁶ They suspected that icetexone was derived from conacytone due to the similarities in structure. However, this synthetic link was not confirmed until several years later.

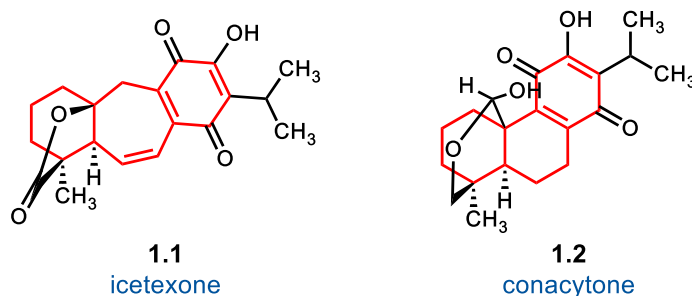


Figure 1.1 First discovered icetexone

Since the seminal isolation of icetexone in 1976 by Watson and coworkers, over 150 different icetexane natural products have been described. Icetexanes have been shown to have a variety of biological activities ranging from antimicrobial (lanigerol **1.3**),⁷ antibacterial (salviasperanol **1.4**),⁸ trypanocidal((+)-komaroviquinone **1.5**),⁹ antiproliferative, and cytotoxic activities (**1.6** and salviadenone A **1.7**).^{2,10,11}

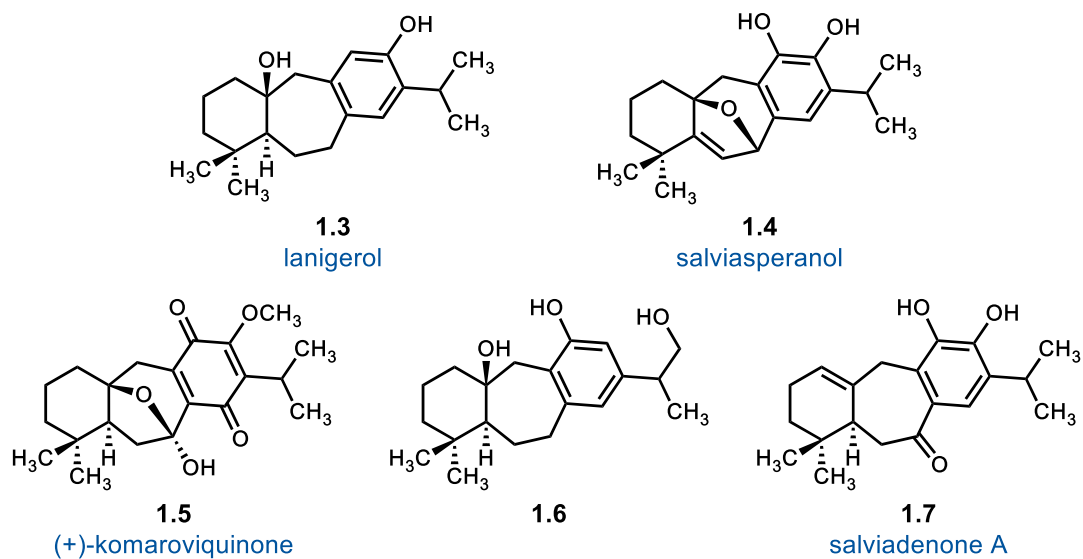


Figure 1.2 Some icetexane natural products

1.2 Classification

There are currently six classes of icetexanes that indicate both the regiochemistry and degree of oxygenation of the core scaffold. In 2009, Simmons and Sarpong proposed an icetexane classification system based upon the position of oxygenations on the 6–7–6 tricyclic scaffold. Their five proposed classes involved variations in oxygenations about C(3), C(11), C(12), C(14), and C(19).^{10c} An additional sixth class that did not fall within the icetexane classes described by Simmons was proposed by the Chain group in 2022 to account for novel icetexanes isolated after the 2009 review.^{10b}

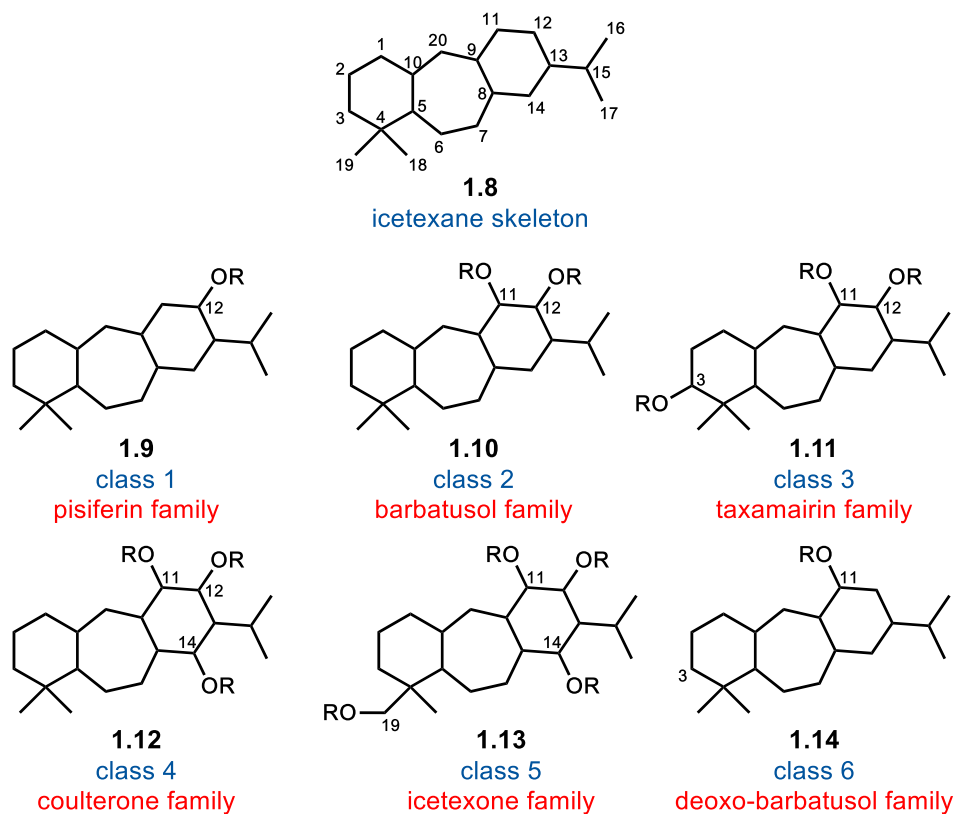


Figure 1.3 Icetexane classification

Icetexane class 1 **1.9** is oxygenated solely at C(12). Members of this class are named after the natural product pisiferin **1.15**, which was first isolated from the leaves of *Chamaecyparis pisifera*.¹² Originally thought to contain a 7–6–6 tricyclic framework, the correct structure of pisiferin was elucidated by a second isolation from the seeds of *Chamaecyparis pisifera*.¹³

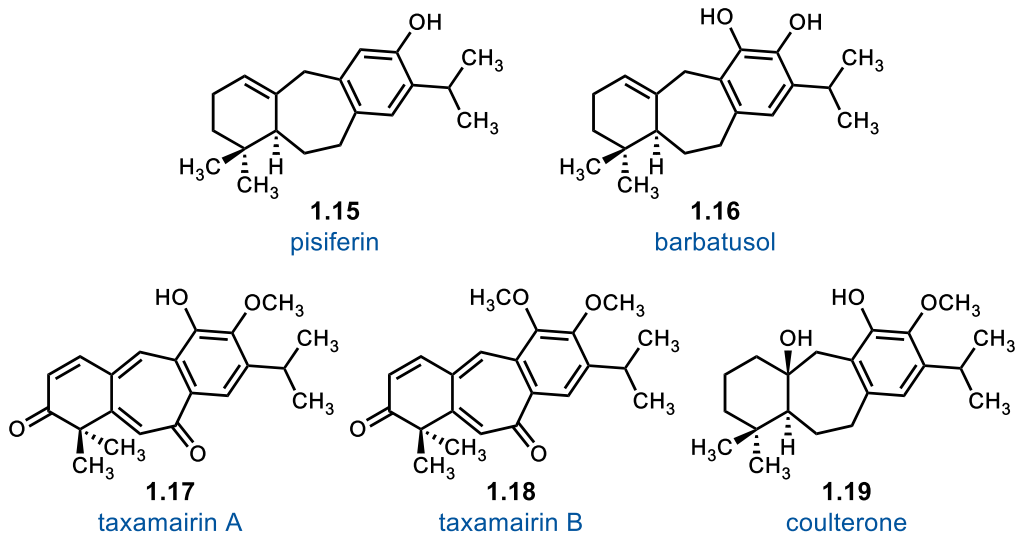


Figure 1.4 Parents of icetexane classes

IceTexane class 2 **1.10** is oxygenated at both C(11) and C(12). Members of this class are named after the natural product barbatusol **1.16**, which was first isolated from the bark and heartwood of *Coleus barbatus*.¹⁴ The structural elucidation of barbatusol helped to establish the biosynthetic relationship between abietanes and icetexanes.

IceTexane class 3 is oxygenated at C(3), C(11), and C(12). Members of this class are named after the natural products taxamairin A **1.17** and taxamairin B **1.18**, which were both isolated from the bark of *Taxus mairei*.¹⁵

IceTexane class 4 is oxygenated at C(11), C(12) and C(14). Members of this class are named after the natural product coulterone **1.19**, which was first isolated from roots of *Salvia coulteri*.¹⁶

IceTexane class 5 is oxygenated at C(11), C(12), C(14) and C(19). Members of this class are named after icetexone **1.1**, the first icetexane to be discovered.⁶

IceTexane class 6 is oxygenated solely at C(11). Because members of this class lack the second oxygenation at C(12) characteristic of barbatusol, icetexane class 6 is designated as the

deoxo-barbatusol family. The first class 6 icetexanes were isolated alongside barbatusol icetexanes by Rao and coworkers in 2009 year from the stem bark of *Premna tomentosa*.¹⁷

1.3 Biosynthetic Pathway

IceTexanes are found in plants that often produce abietane natural products and are thought to be related as secondary metabolites. Abietane natural products, with a 6–6–6 tricyclic framework **1.20**, are thought to rearrange into the resulting 6–7–6 tricyclic framework of icetexanes **1.8** which therefore bears the systematic name 9(10 →20)-abeo-abietane.¹⁷

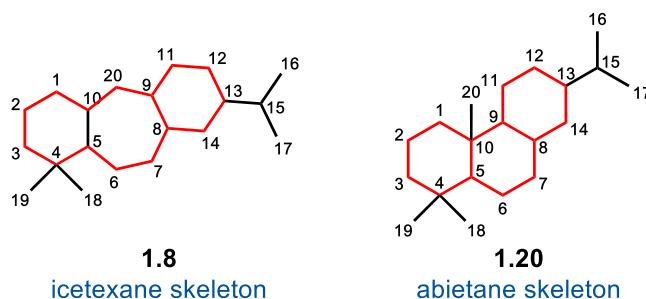


Figure 1.5 Comparison of the icetexane and abietane frameworks

The first link between icetexanes and abietanes was discovered by Rodriguez-Hahn and coworkers in 1983.¹⁸ They discovered that treating abietane **1.21** with potassium carbonate and iodomethane in wet acetone resulted in the opening of the lactone moiety and formation of a C(6)–C(7) double bond to afford ester **1.22**. Subsequent hydrogenation and reduction generated the primary alcohol **1.23**. Treatment of alcohol **1.24** with an excess amount of 4-toluenesulfonyl chloride in pyridine generated barbatusol dimethyl ether **1.25**.

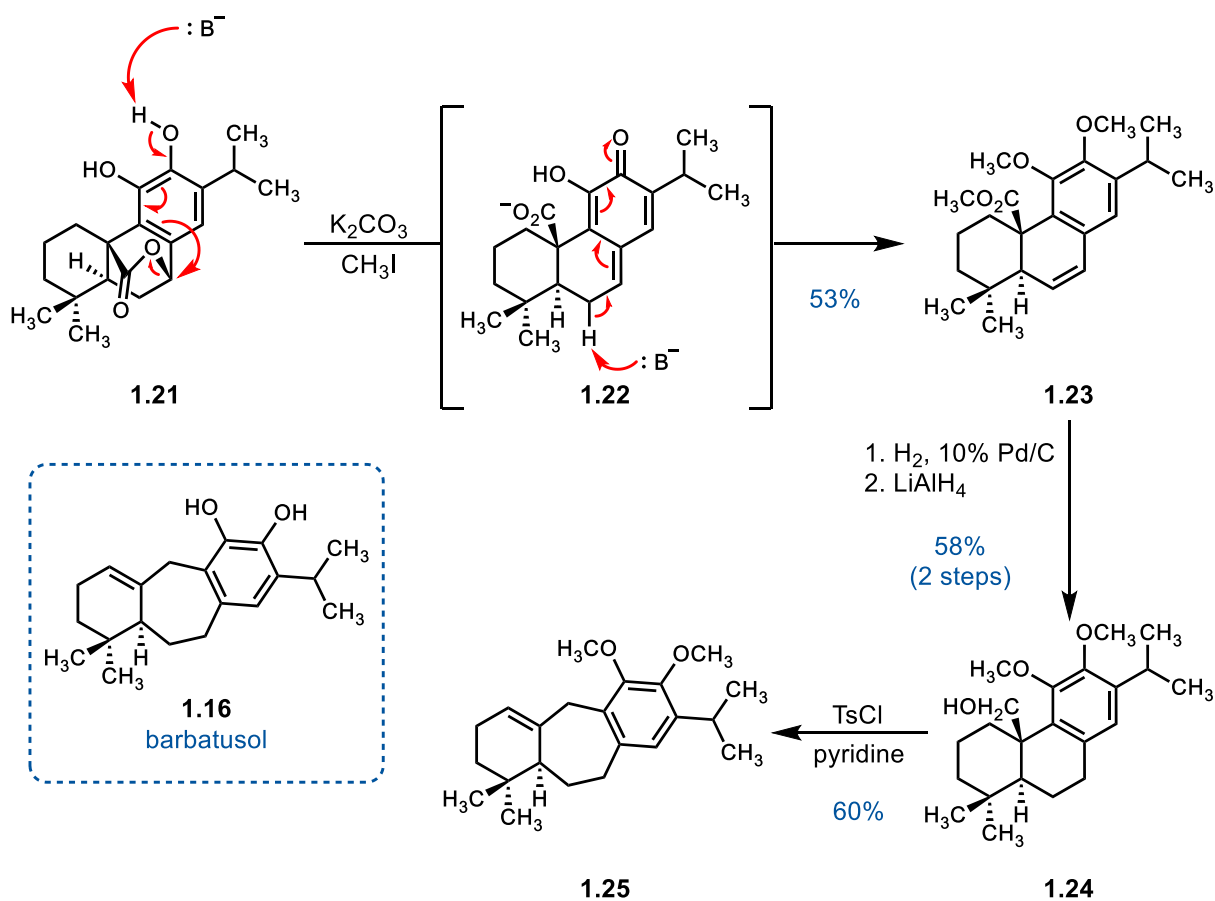


Figure 1.6 First discovered synthetic link between abietanes and icetexanes

In 1991, Gonzalez and coworkers proposed a general biosynthetic pathway from abietanes to icetexanes.¹⁹ It began with an enzymatic protonation–dehydration of **1.26**, yielding intermediate **1.27**. Intermediate **1.27** then undergoes a Wagner–Meerwein rearrangement to produce carbocation intermediate **1.28**, which now contains the central 7–member ring of the icetexanes. **1.29** is then obtained by trapping the carbocation **1.28** by water. It has also been reported that the C(20) activated abietane **1.27** could be a result of enzymatic hydride abstraction from the C(20) methyl group of the abietane **1.30**, which then undergoes the aforementioned carbocation cascade to generate icetexane natural products.²⁰

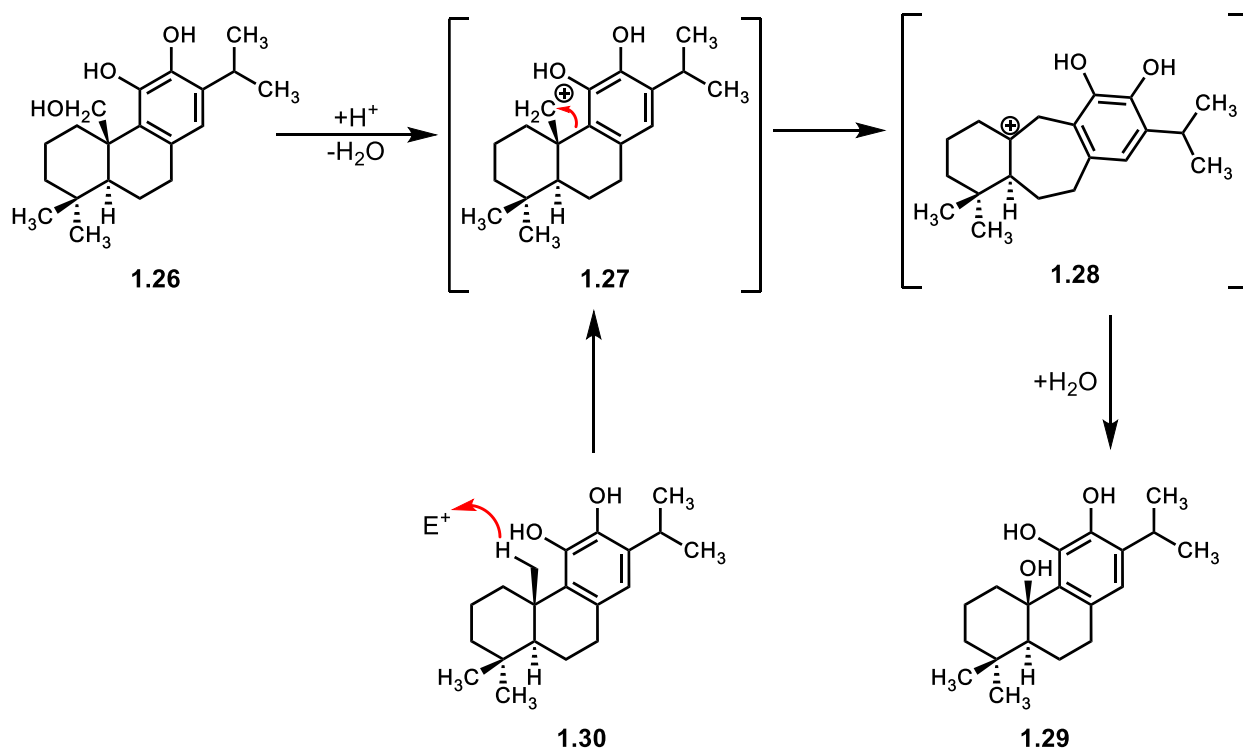


Figure 1.7 Biosynthetic pathway from abietanes to icetexanes

1.4 Early Synthetic Milestones

Icetexanes first appeared in literature in 1976 with the seminal isolation of icetexone **1.1** from the *Salvia Ballotaeflora* by Watson and coworkers.⁶ Just ten years later, Matsumoto and coworkers reported the first total synthesis of a racemic icetexane, pisiferin **1.15**.²¹ It began with a Wittig reaction to join phosphonium ylide **1.31** and racemic aldehyde **1.32**, followed by a selective hydrogenation of the resulting styrene to produce the trisubstituted aromatic **1.33**.²² Epoxidation of **1.33** with *m*-chloroperbenzoic acid (*m*CPBA) and the subsequent epoxide opening under the action of lithium *N,N*-diethylamide (LiNEt₂) afforded alcohol **1.34**.²³ Alcohol **1.34** was oxidized to the corresponding enone under the action of pyridinium chlorochromate (PCC) and then cyclized upon heating at 80–85 °C with polyphosphoric acid to generate a mixture of epimeric

ketones **1.35a** and **1.35b**. Ketone **1.34** was then reduced with lithium aluminum hydride (LiAlH₄) and demethylated to afford alcohol **1.36**. Alcohol **1.36** was regioselectively dehydrated by bimesylation and followed by heating in 2,4-lutidine to give the alkene **1.37**, which was then demesylated under the action of LiAlH₄ to generate racemic pisiferin **1.15**.

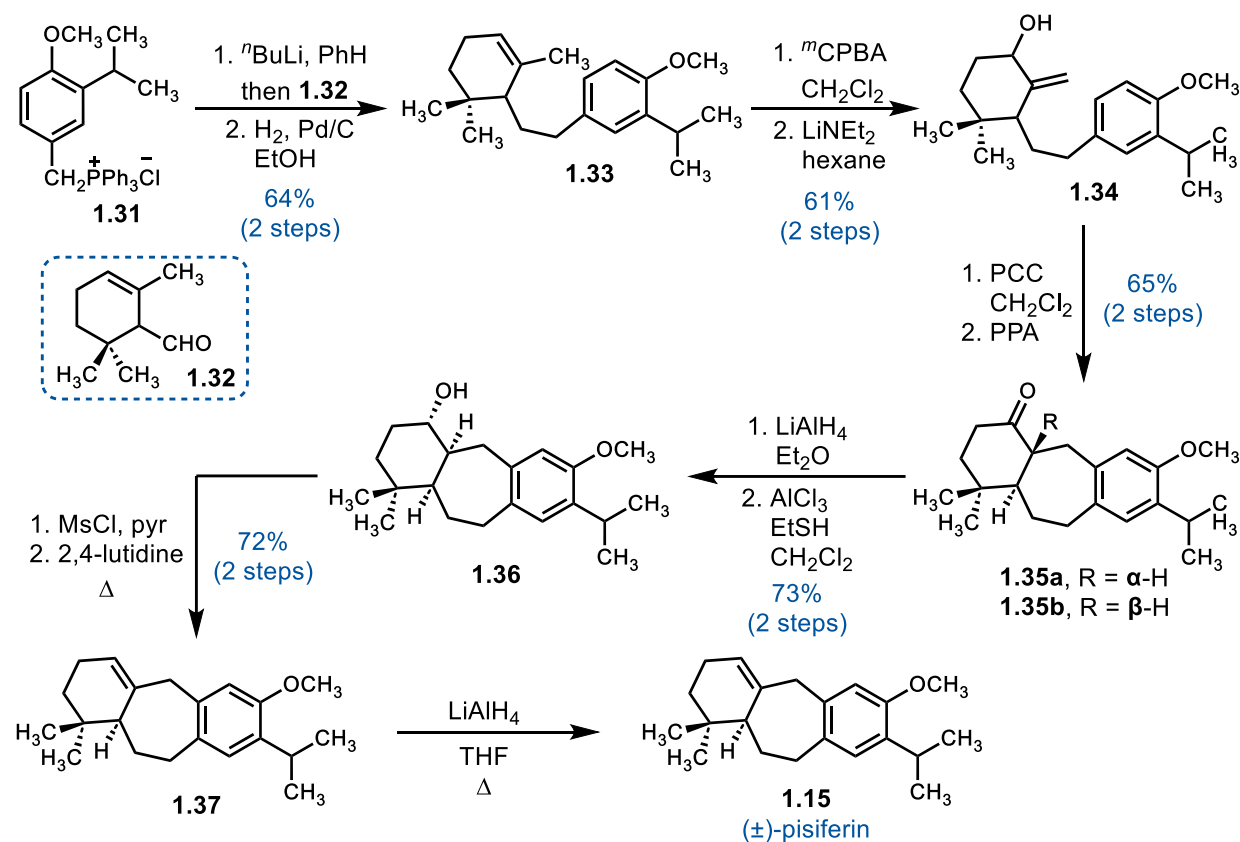


Figure 1.8 Synthetic route to pisiferin **1.15**

The first asymmetric total synthesis of an icetexane, (+)-komaroviquinone **1.5**, was completed by Majetich's group in 2007.²⁴ The synthesis began with an eight-step preparation of benzyl bromide **1.39** from 3,4,5-trimethoxybenzoic acid. Diketone **1.38** was deprotonated under the action of sodium hydride and the corresponding enolate was alkylated with bromide **1.39** before a second enolization event and *O*-methylation with dimethyl sulfate occur to afford enone **1.40**. Enone **1.40** then underwent a tandem Isler²⁵ alkylation–Stork–Danheiser²⁶ transposition

to afford enynone **1.41**. Lindlar reduction of **1.41** afforded conjugated dienone **1.42**, which was then cyclized under the action of a Lewis acid to afford the tricyclic icetexane product **1.43**.²⁷ Bromination of **1.43** with *N*-bromosuccinimide (NBS) in acetic acid followed by a radical dehalogenation and a stereoselective reduction with the Corey-Bakshi-Shibata catalyst generated acetates **1.44** as a 1 : 1 diastereoisomeric mixture.²⁸ Acetate **1.45** undergoes a Myers allylic transposition followed by a two-step acetate cleavage-oxidation sequence to afford ketoalkene **1.46**.²⁹ Introducing NBS in wet acetone to the ketoalkene **1.46** followed by radical dehalogenation generated **1.47** which upon oxidation under the action of silver(II) oxide in 7 N nitric acid afforded (+)-komaroviquinone **1.5**.⁹

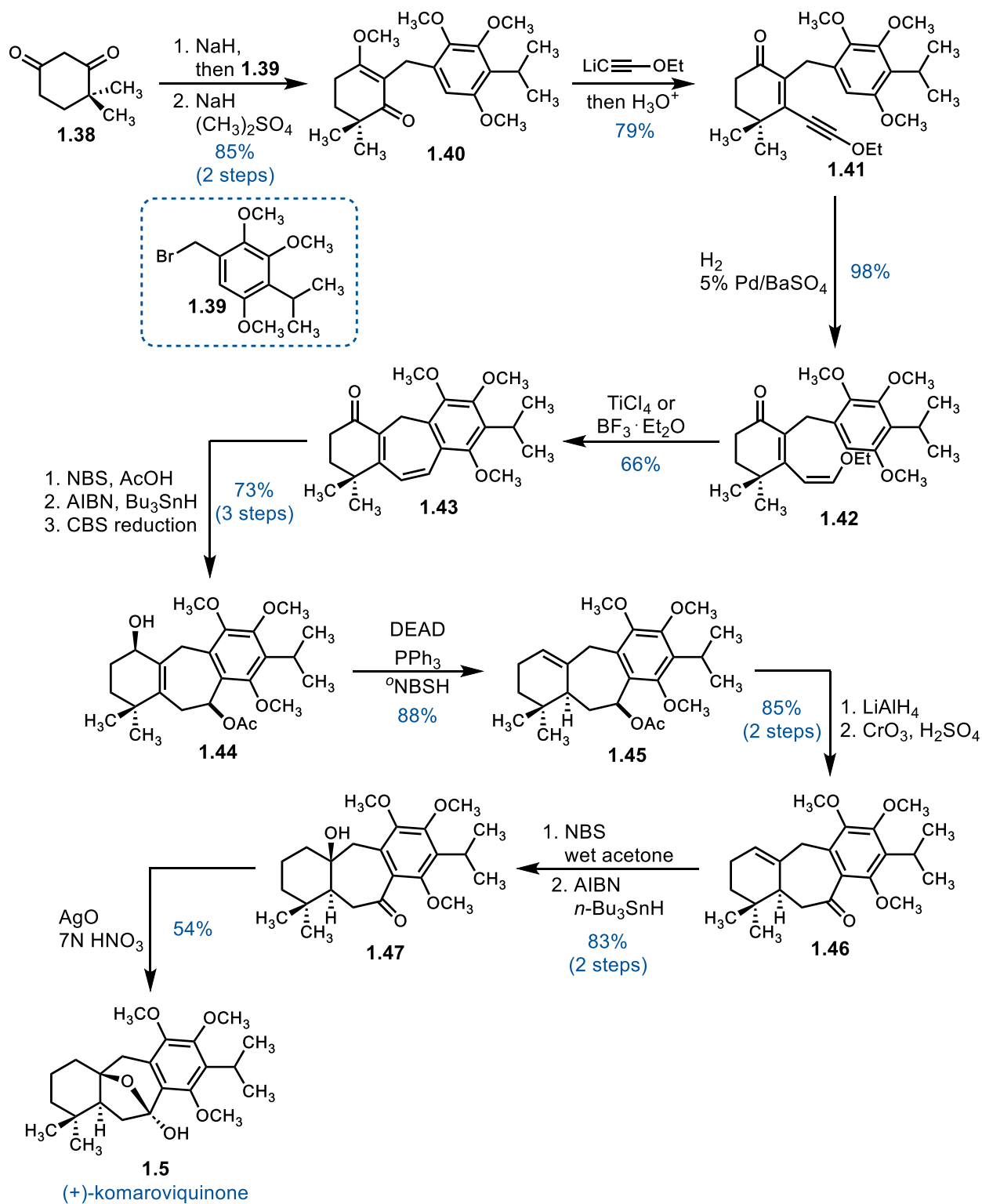


Figure 1.9 Synthetic route to komaroviquinone **1.5**

CHAPTER 2

Premnalatifolin A & Synthesis of Icetexane Analog Intermediates

2.1 Introduction to Premnalatifolin A

Several plants belonging to the genus *Premna* have been used for treatment of hepatic disorders and for antioxidant and immunomodulatory effects; in particular *Premna latifolia* is commonly used in many traditional medicine treatments in India. *Premna latifolia* Roxb. is more commonly called Agnimantha and Arani and is known to be medicinally potent and a rich source of antioxidants.³⁰ The bark of *Premna latifolia* Roxb. is traditionally ground into a paste and applied to cure boils.³¹ Its leaves have diuretic, anti-inflammatory, and anti-cancerous properties.^{4,31} The plant is used to treat a variety of ailments, including diarrhea, beri-beri, vaginal irritation, snakebites, liver ailments, ulcers, hemorrhoids, indigestion, and cough.³²

One isolated icetexane of interest is the heterodimeric diterpene icetexane premnalatifolin A **2.1**. Premnalatifolin A was isolated in 2011 by Babu and co-workers from the stem bark extracts of the *Premna latifolia*, along with three monomeric icetexanes latifolionol **2.2**, dihydrolatifolionol **2.3**, and latiferanol **2.4**.³³

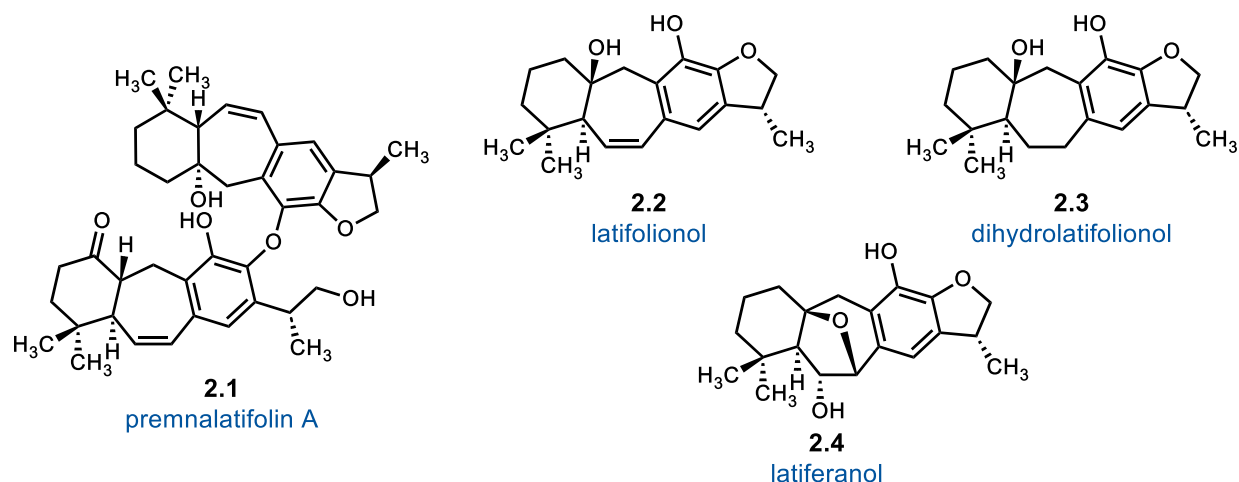


Figure 2.1 Structures of icetexanes isolated from *Premna latifolia*

Of the aforementioned icetexanes isolated from *Premna latifolia*, Premnalatifolin A and latifolionol were shown to be active against breast cancer and colon cancer cell lines when tested against eight human cancer cell lines. Premnalatifolin A and latifolionol exhibit an $IC_{50} = 1.77 \mu\text{M}$ and $IC_{50} = 3.53 \mu\text{M}$ against MCF-7 breast cancer cell lines, respectively.^{33,34} Premnalatifolin A and latifolionol also exhibit an $IC_{50} = 19.4 \mu\text{M}$ and $IC_{50} = 127 \mu\text{M}$ against HT-29 cell lines, respectively. In comparison, the industry standard of care for breast cancer patients, Doxorubicin (Adriamycin®), has an IC_{50} of $3.70 \mu\text{M}$ against MCF-7 cancer cell lines.³⁵ Unfortunately, Doxorubicin earned the nickname “the red death” due to the severe deleterious side effects, acute cardiotoxicity, and high rates of fatalities. The undesired side effects of Doxorubicin and biological activity profile of Premnalatifolin A make for a promising candidate for alternative chemotherapeutic therapies for breast cancer patients.

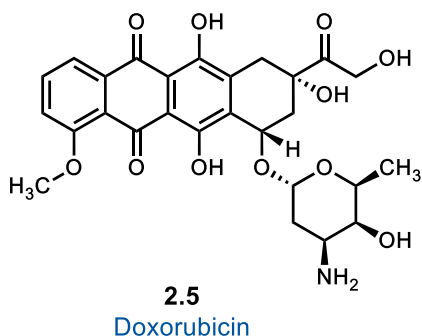


Figure 2.2 Structure of doxorubicin

2.2 Prior Synthesis Studies

In 2018, a simple strategy towards the synthesis of simple monomeric analogues of premnalatifolin A was developed in Prof. William Chain's laboratories. The synthesis proceeds with the joining of two key intermediates, silylenol ether **2.7** or **2.9**, and benzyl chloride **2.12**. The synthesis of the silylenol ether **2.7** began with a Michael 1,4 Addition of 2-cyclohexen-1-one **2.6** and vinylmagnesium bromide in the presence of copper(I) iodide and the resultant enolate is trapped with chlorotrimethylsilane in 96% yield.³⁶

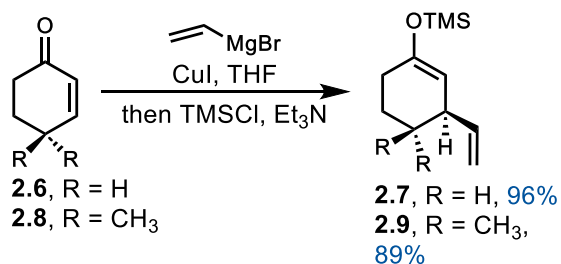


Figure 2.3 Synthetic route to silylenol ether **2.7** and **2.9**

The benzyl chloride **2.12** was synthesized in five steps. A nucleophilic aromatic substitution with potassium hydroxide and 2-chloro-6-fluorobenzaldehyde **2.10** gave the

corresponding chlorosalicylic acid in 91% yield,³⁷ which then underwent a Suzuki-Miyaura coupling with potassium vinyltrifluoroborate under the action of palladium(II) acetate with (±)-BINAP as ligand in dimethylformamide/water to give the styrenealdehyde **2.11** in 93% yield.³⁸ The aldehyde was then converted to benzyl chloride **2.12** over three steps via silyl protection, reduction of the aldehyde and conversion of the resultant alcohol, with a 79% overall yield.

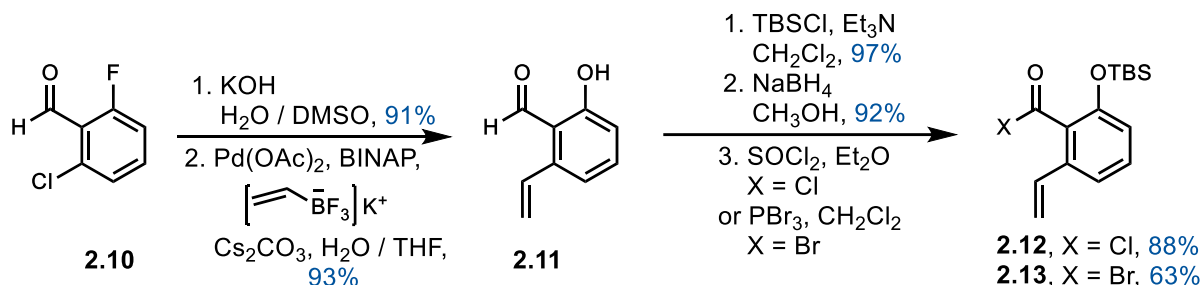


Figure 2.4 Synthetic route of benzyl chloride **2.13**

Initial attempts to join the two key intermediates were made using the enolate-ortho-quinone-methide (OQM) coupling sequence developed in the Chain group.³⁹ This was first tested on a simplified model system with silylenol ether **2.7** and silyloxy benzyl chloride **2.12**. It was found that silylenol ether **2.7** and silyloxy benzyl chloride **2.12** joined together quickly and diastereoselectively to exclusively afford the 1,2-trans alkylation product **2.14**. However, there also was a post-alkylation addition of the phenoxide to the carbonyl function to give cyclic hemiketal diastereomers **2.15**. The open ketophenol **2.14** could not be captured using the OQM reaction strategy, even upon many efforts to open the resultant cyclic hemiketal.

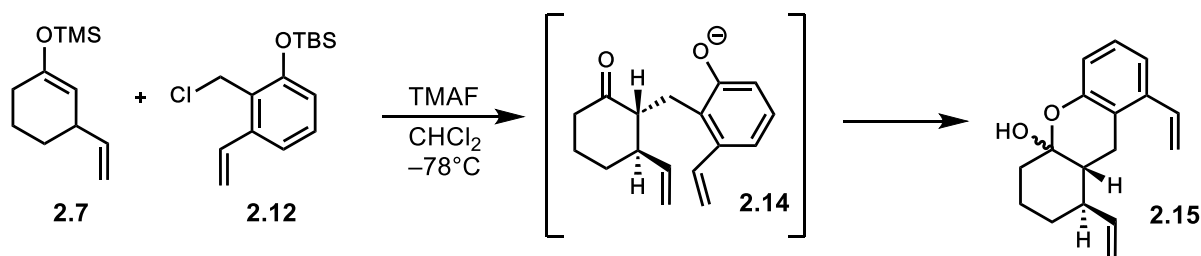


Figure 2.5 Unsuccessful alkylation via the OQM methodology

Other efforts to form the carbon–carbon bond linkage were then explored. Treatment of the silylenol ether **2.7** with methyllithium in dimethyl ether at -78°C unmasked the silyl enolate to allow for the alkylation of benzyl chloride intermediate **2.12**. The alkylation proceeds diastereoselectively and afforded the desired product **2.16** in 35% yield. **2.17** could also be synthesized in 75% yield by implementing 4,4-dimethyl-2-cyclohexen-1-one as the silyl enol ether precursor. **2.16** and **2.17** alkylations both resulted in the formation of second regioisomers, likely as a result of isomerization of the enolate during the reaction conditions. Subsequently, the vinyl groups were joined in ring-closing metathesis reactions utilizing Grubbs second generation catalyst **2.18** in dichloromethane to give the corresponding protected icetexanes **2.19** and **2.20** in 92% and 85% yield, respectively.⁴⁰ With the protected core 6–7–6 tricyclic framework in place, **2.19** and **2.20** were hydrogenated using palladium on carbon in ethyl acetate to give **2.23** and **2.24**. Analogues **2.19**, **2.20**, **2.23** and **2.24** were deprotected using tetrabutylammonium fluoride in tetrahydrofuran at 23°C to give ketophenols **2.21**, **2.22**, **2.25** and **2.26** with yields of 73%, 53%, 71%, and 99%, respectively.

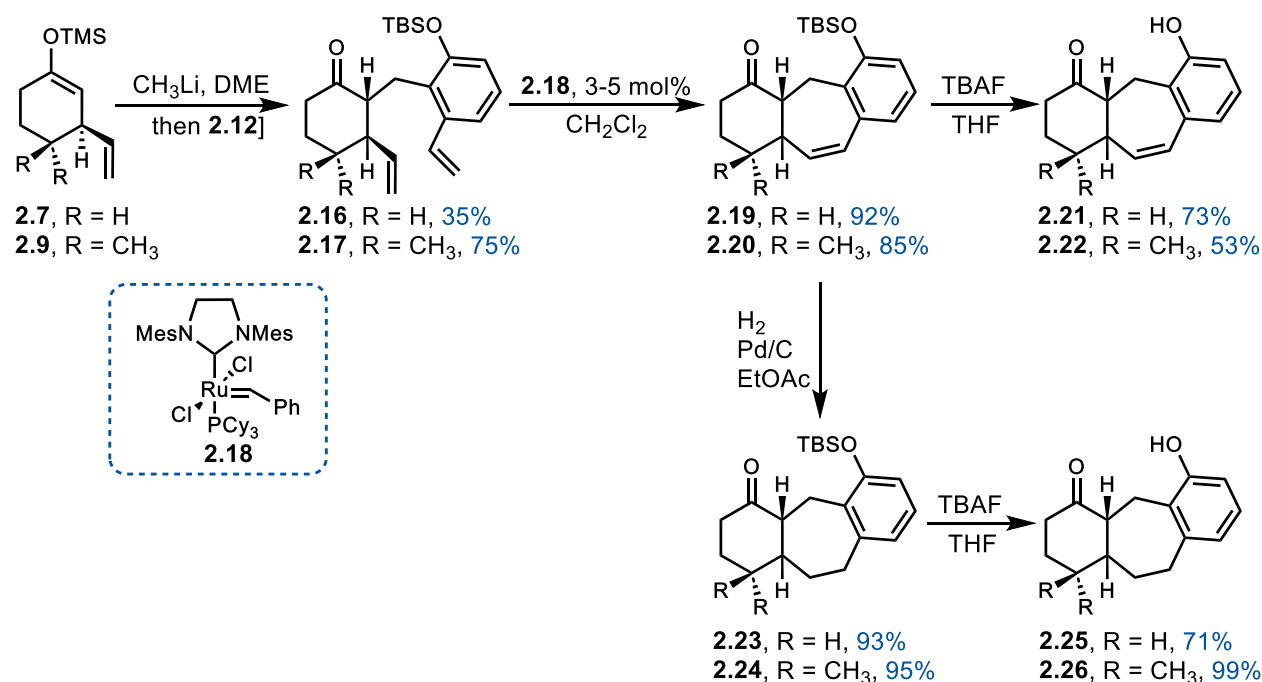


Figure 2.6 Synthetic routes to icetexanes **2.21**, **2.22**, **2.25** and **2.26**

Of these four icetexane analogues, **2.25** was soluble in cell media culture and viable for testing against the MCF-7 breast cancer cell line. Increasing concentrations of **2.25** decreased the cell survival of MCF-7 and the LD₅₀ was determined to be 250 μ M. Encouraged by this LD₅₀, it was determined that alternative icetexane analogues with both increased biological activity towards tumor cells and low cytotoxicity are therefore desirable. Additionally, the low water solubility of analogues **2.21**, **2.22**, **2.25** and **2.26** necessitates the generation of new analogues containing additional functional groups to improve water solubility and increase potency.

Inspired by the works of Moon et. al., Dr. Ali Amiri Naeini first targeted the synthesis of diol **2.27** to address the low water solubility of **2.22**.

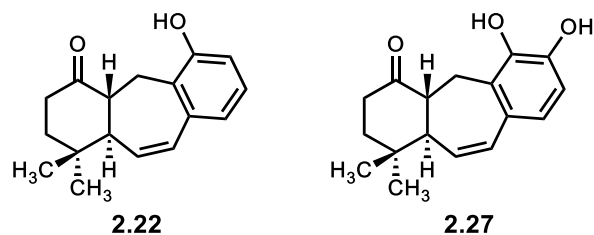


Figure 2.7 Structural comparison of targeted icetexanes **2.22** and **2.27**

Tetrasubstituted aromatic **2.29** was synthesized from 2,3-dihydroxybenzaldehyde from previously described literature procedures.⁴¹ **2.29** then underwent a Suzuki-Miyaura reaction under basic conditions to give **2.30**.⁴²

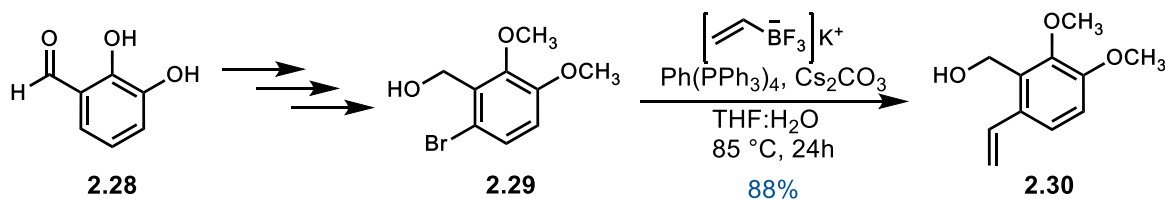


Figure 2.8 Synthetic route to **2.30**

The benzylic alcohol on **2.30** was converted to the corresponding bromine in a two-step one-pot process. The alcohol is first converted to the corresponding methylsulfonate under the action of triethylamine and methanesulfonyl chloride followed by displacement of the resultant mesylate with lithium bromide to afford the benzyl bromide **2.31**.⁴³ The silyl enol ether **2.9** is then treated with methyl lithium to unmask the trimethylsilyl group and reveal lithium enolate. The alkylation reaction is then performed following the precedent set by Moon et. al. **2.31** is added to the lithium enolate to afford **2.32a** and its regioisomer **2.32b**. The resulting regioisomeric mixture was then subjected to the Grubbs Catalyst 2nd Generation in a final ring closing metathesis reaction

to afford the icetexane **3.33** (40% over three steps), as only the desired regioisomer of the alkylation undergoes ring closing metathesis.⁴⁴ Alex Ziegelmeier then completed the synthesis of diol **3.27** by treating icetexane **3.33** with boron tribromide (BBr₃) to afford diol **3.27**.

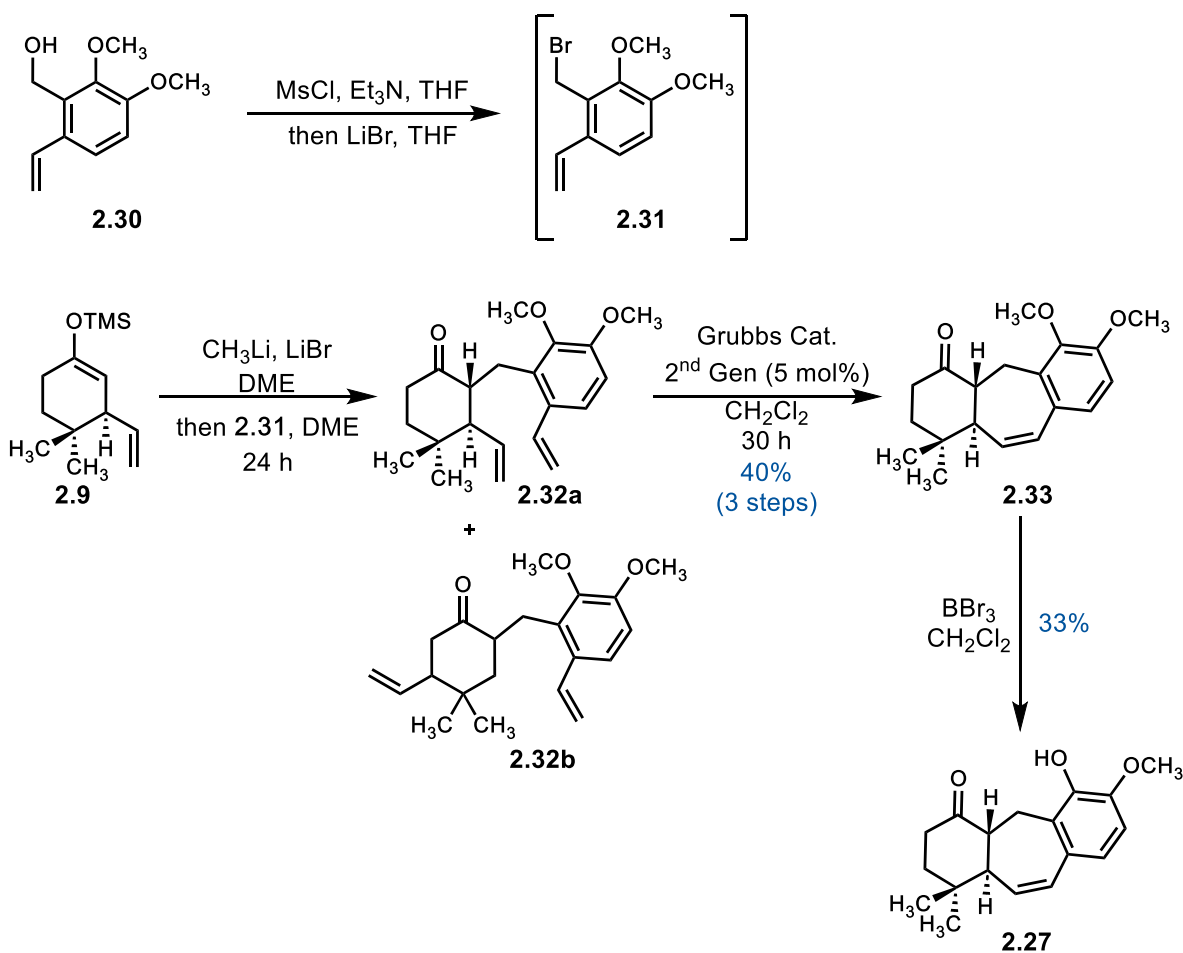


Figure 2.9 Synthetic route to icetexane **2.27**

2.3 Synthetic Efforts towards the Southern Monomer of Premnatifolin A

The Chain group at the University of Delaware first focused on synthesizing the southern monomer of premnatifolin A applying the knowledge gained from the construction of the simplified analogs. The Chain group strategy towards synthesizing icetexanes involves the joining of a cyclohexanone enolate nucleophile with highly functionalized benzyl halide electrophile.

Naeini encountered difficulties in the formylation of tetrasubstituted aromatic species to generate the precursor for alkylation. Despite extensive efforts, Naeini was initially unable to formylate rapidly generated tetrasubstituted aromatics utilizing the Rieche or Vilsmeier–Haack protocols.⁴⁵

He was eventually able to access pentasubstituted aromatic **2.46** through a lengthy synthesis. Benzaldehyde **2.34** was treated with boron tribromide followed by methyl iodide and potassium carbonate to shuffle the methyl group from one phenol to the other to afford **2.35**. Benzaldehyde **2.35** was oxidized to a carboxylic acid utilizing Tollens' oxidation protocol and then esterified under acidic conditions to afford benzylic ester **2.36**.⁴⁶ Benzylic ester **2.36** was converted to tertiary alcohol **2.37** under the action of two equivalents of methyl magnesium bromide. Tertiary alcohol **2.37** was dehydrated by pyridinium *p*-toluenesulfonate to afford styrene **2.38** which then underwent a hydroboration–oxidation protocol to yield primary alcohol **2.39**. The phenolic hydroxyl on **2.39** was allylated to generate **2.40** which was then methylated to afford *O*-allylbenzene **2.41**. Treatment of *O*-allylbenzene **2.41** with heat resulted in a Claisen [3,3]-sigmatropic rearrangement to afford allylbenzene **2.42**.

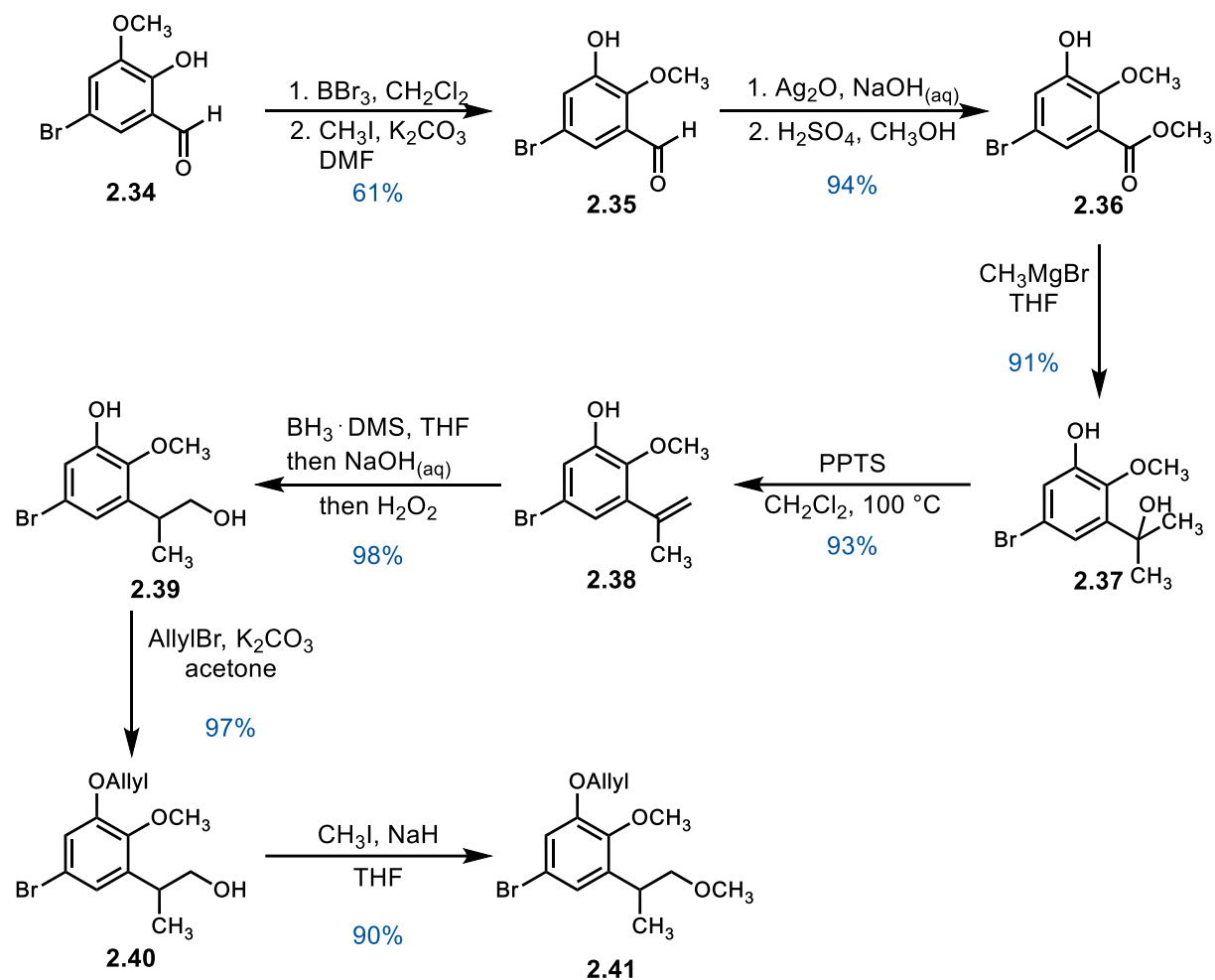


Figure 2.10 Synthetic route to allylbenzene **2.41**

Allylbenzene **2.42** was isomerized under basic conditions to yield a styrene and subsequently trapped with methyl iodide to afford **2.43**. **2.43** then underwent a reductive ozonolysis to produce benzaldehyde **2.44** which was then subjected to a Suzuki-Miyaura coupling to afford styrene **2.45**. Reduction of styrene **2.45** with diisobutylaluminium hydride generated the desired pentasubstituted righthand side of the southern monomer, **2.46**.

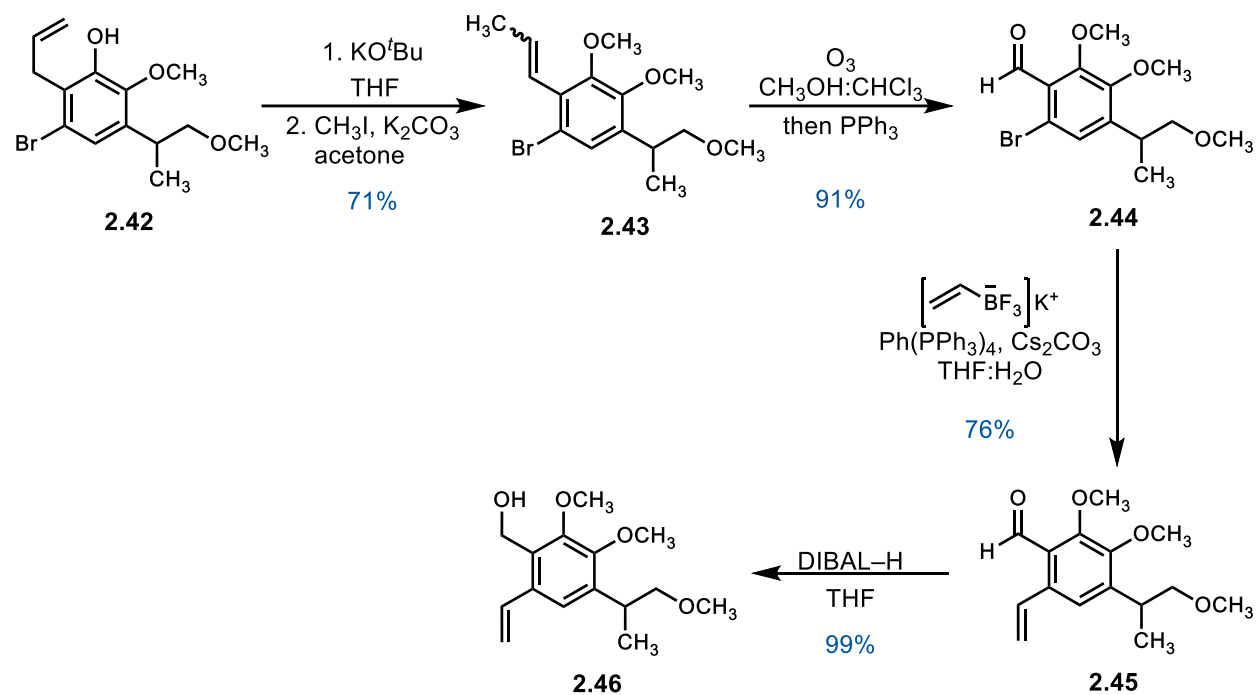


Figure 2.11 Synthetic route to the righthand side of the southern monomer, **2.46**

The joining of the right- **2.9** and lefthand **2.46** sides of the southern monomer was achieved using previously employed methods to produce icetexane **2.49**.

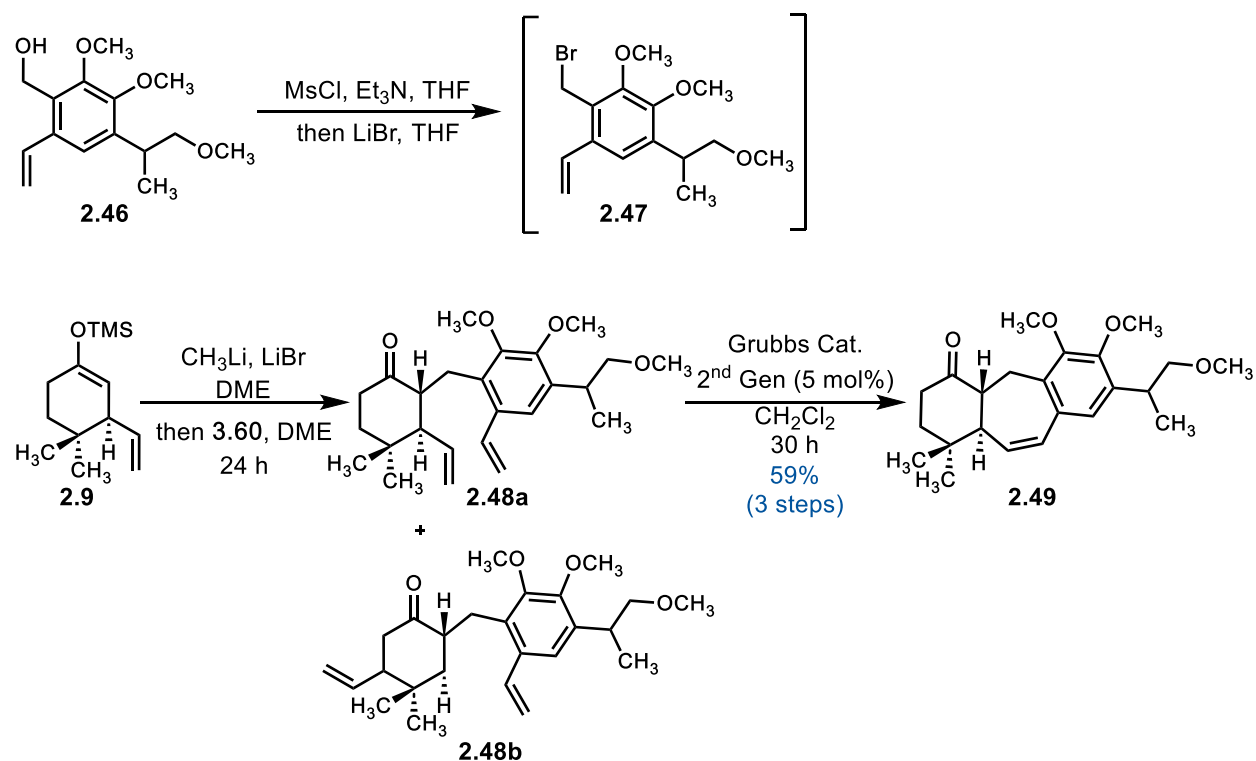


Figure 2.12 Synthetic route to icetexane **2.49**

Alex Ziegelmeier built upon Naeini's work to complete the protected southern monomer of Premnatifolin A. To this end, **2.50** was synthesized from **2.34** with their *tert*-butyldimethylsilyl (TBS) alcohol projective groups over 16 steps. I have previously assisted in the completion of this synthesis of **2.50** during work completed before my thesis project. The same alkylation and ring-closing metathesis strategy utilized by Naeini to join enolate **2.9** and vinyl bromide **2.51**, Ziegelmeier was able to synthesize **2.53**. However, the previously described deprotection strategy with BBr_3 not only fully stripped **2.53** of their respective protecting groups but also brominated at the end of the alkyl chain. This undesired bromination led to the attempts of other global deprotection conditions but also yielded no success. Due to the lengthy synthesis of **2.53** and **2.49** and difficulty of deprotection, a more efficient route to synthesize **2.50** and **2.46** was necessary and is currently under development.

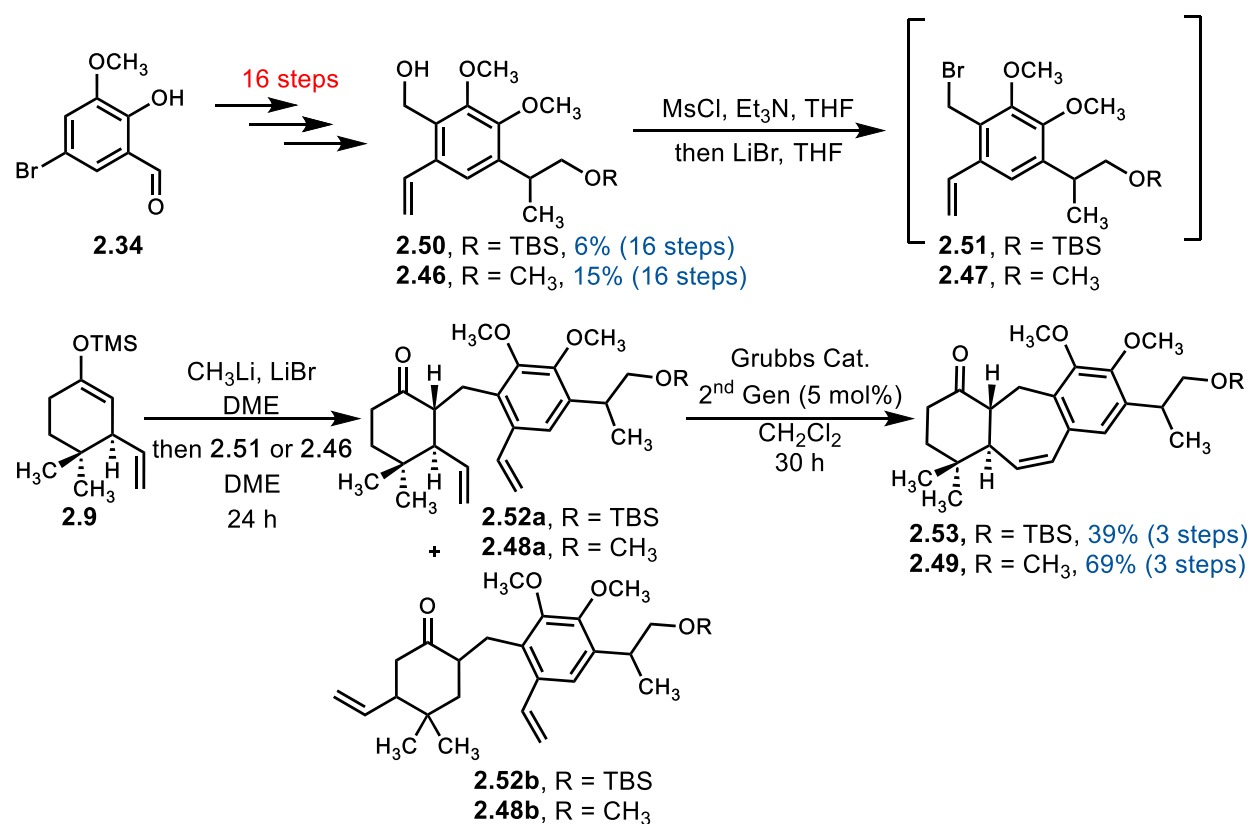


Figure 2.13 Synthetic route to icetexane **2.53**

Ziegelmeier is currently pursuing a more efficient route from **2.34** to **2.50** and **2.46** that leverages an electrochemical pyridinium cross coupling approach to install the alkyl chain at the bromine. Using conditions developed in collaboration with Prof. Mary Watson and her group, **2.54** and **2.58** were subjected to electrolysis using Co (+) and SS (—) electrodes, nickel catalysts, and a pyridinium salt to form **2.55** and **2.59**, respectively.⁴⁷ The syntheses of **2.57** and **2.61** from **2.28** and **2.60** are now viable in seven and five steps, respectively. This chemistry optimizes the number of steps required to synthesize **2.57** from 16 to seven steps, cutting the route down by over half the steps.

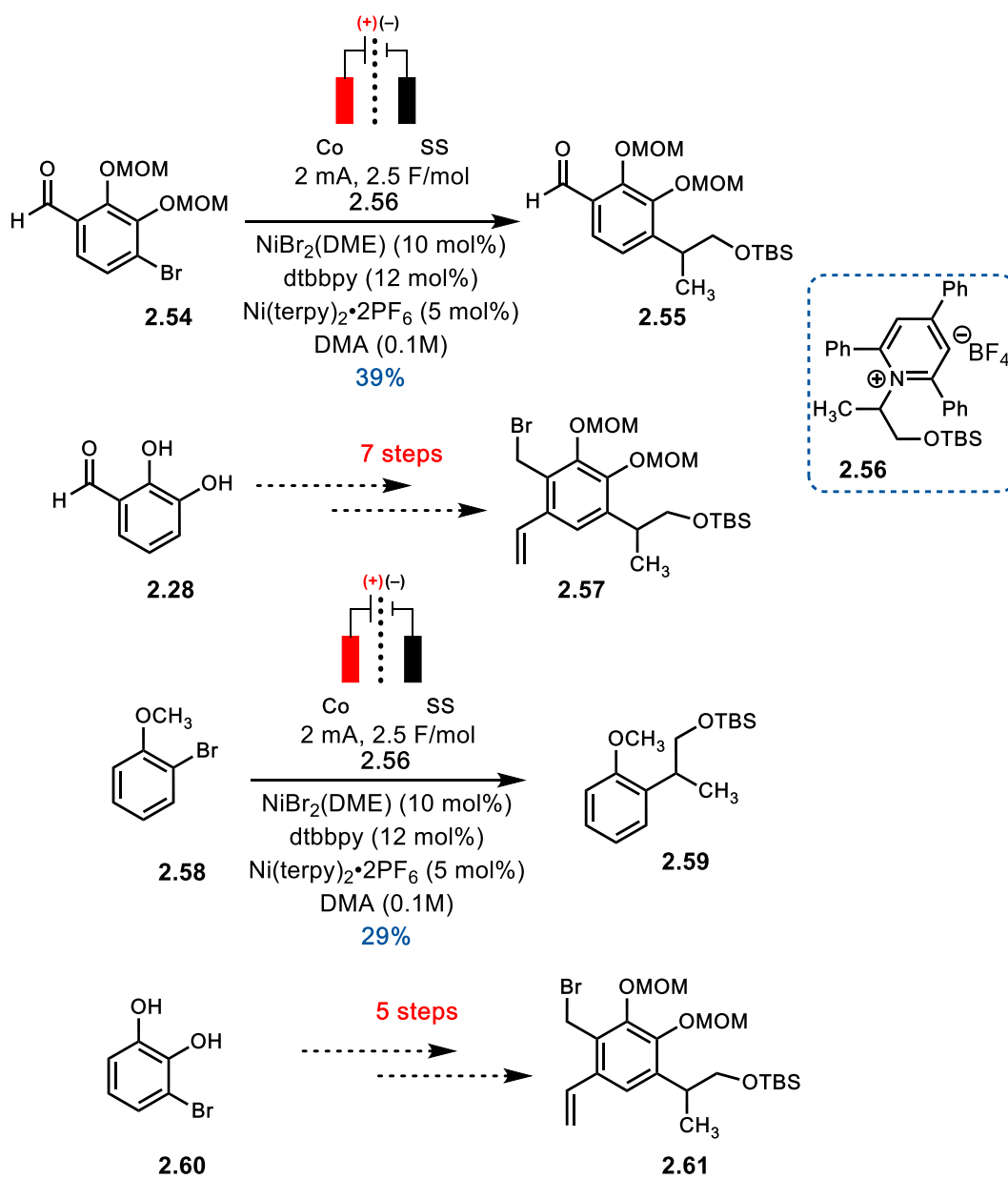


Figure 2.14 Optimization of the route to **2.57**

Ziegemeier was also able to optimize the alkylation conditions, ultimately finding that the reaction proceeded diastereoselectively under the action of tetramethylammonium fluoride, eliminating the formation of the undesired regiosomeric product of the alkylation.

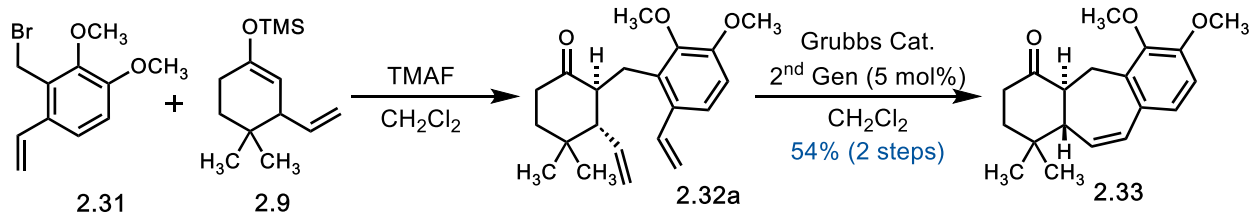


Figure 2.15 Optimization of alkylation conditions

2.4 Synthetic Efforts towards the Northern Monomer of Premnatifolin A

Following the synthesis of the protected southern monomer of premnatifolin A, the Chain group began devising a route towards the northern monomer of premnatifolin A. Unlike the southern monomer, the northern monomer has a dihydrobenzofuran ring connecting C(12) to C(13) and lacks a carbonyl group on C(1), instead carrying a hydroxyl group on C(10). The Chain group proposed a synthetic route involving two key steps: the generation of the dihydrobenzofuran ring and the transposition of the oxygen.

The proposed retrosynthesis first transposes the oxygen in **2.66** through a series of dehydration, epoxidation, and epoxide opening to **2.62**. The dihydrobenzofuran ring **2.3** can then be generated from the open monomer **2.62** via a Mitsunobu type cyclization, or cyclization of the previously mentioned bromide in the synthesis of the southern monomer.⁴⁸

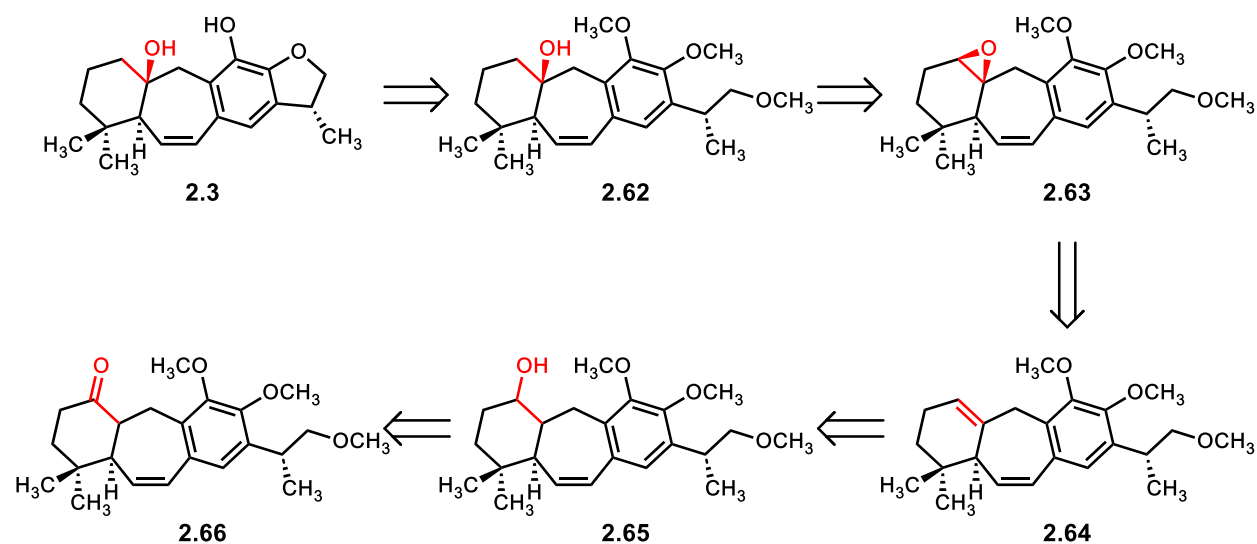


Figure 2.16 Proposed synthetic route to the northern monomer of Premnatifolin A, **2.3**

The success of this route was confirmed using icetexane **2.33** as a model system. Icetexane **2.33** was first reduced under the action of lithium aluminum hydride to give diastereomers **2.67a** and **2.67b**, which were tediously separated.

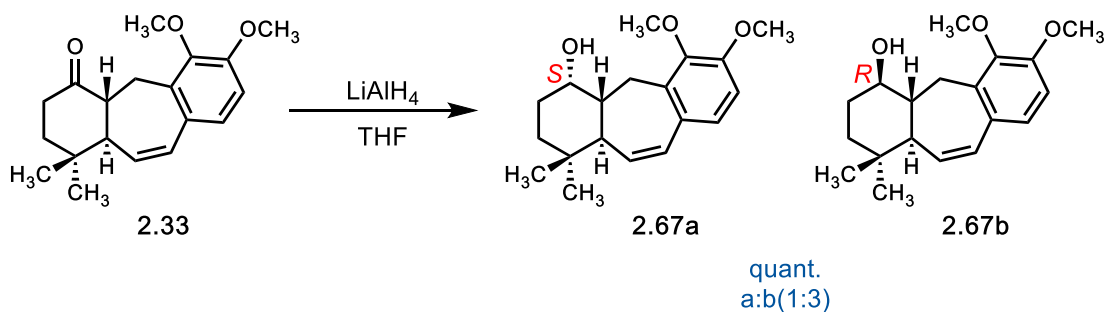


Figure 2.17 Synthetic route to icetexane **2.67**

Diastereomers **2.67a** and **2.67b** were dehydrated to generate diene **2.68** using literature protocols involving treatment with methanesulfonyl chloride in pyridine followed by heating in

2,4-lutidine.²¹ Generation of diene **2.68** from **2.67** was also feasible using the Burgess reagent.⁴⁹

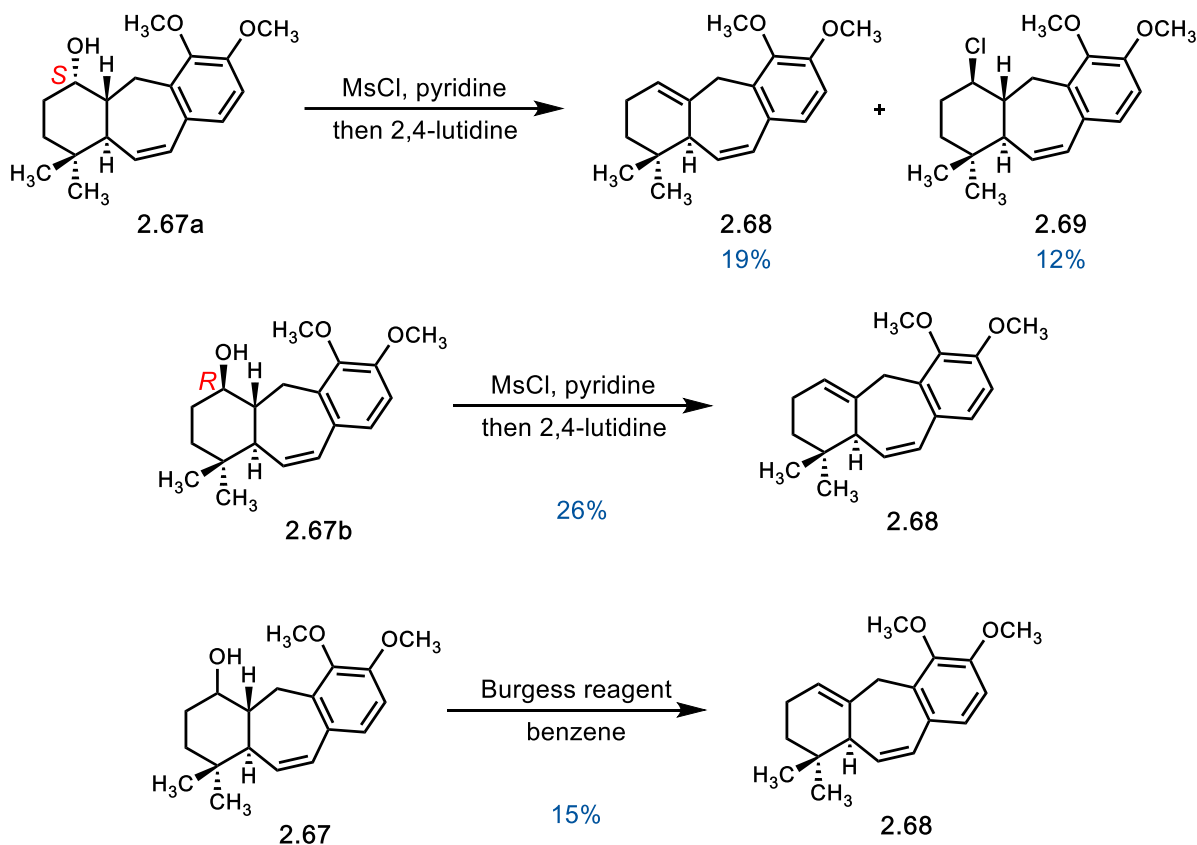


Figure 2.18 Synthetic route to icetexane **2.68**

Diene **2.68** was then epoxidized under the action of *m*-CPBA to form epoxide **2.70**, the stereochemistry of which is currently still under investigation. The northern monomer model **2.71** is then generated through an epoxide ring opening reaction of epoxide **2.70** under the treatment of lithium aluminum hydride.

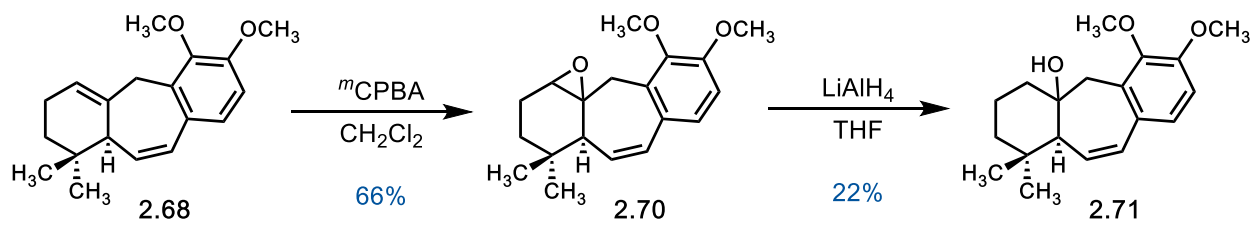


Figure 2.19 Synthetic route to icetexane **2.71**

Further synthetic investigations are necessary to both optimize this route and apply this methodology to other icetexanes in order to access the northern monomer of Premnatifolin A.

CHAPTER 3

Analog Synthesis Routes and Experimentation

3.1 Background and Necessity

More recently, the Chain group is devising a medicinal chemistry approach to synthesize a large array of icetexanes and analogues. As previously demonstrated in simplified scaffolds, the biological activity of an icetexane may be greatly affected by a change in functional groups. The variable functional groups of interest can be seen in **Figure 3.1**.

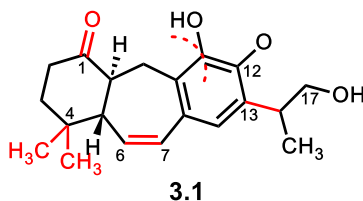


Figure 3.1 Functional groups of interest on icetexanes

One feature of interest is the oxidation state at C(1). The presence or absence of the gem-dimethyl at C(4), the double-bond between C(6) and C(7), and the alkyl group at C(13) are also of interest. In the presence of the alkyl group at C(13), a ring formation between C(17) and the oxygen at C(12) is also of interest. To date, the following analogues **3.2** – **3.8** have been synthesized by Moon, Naeini, and Ziegelmeier.

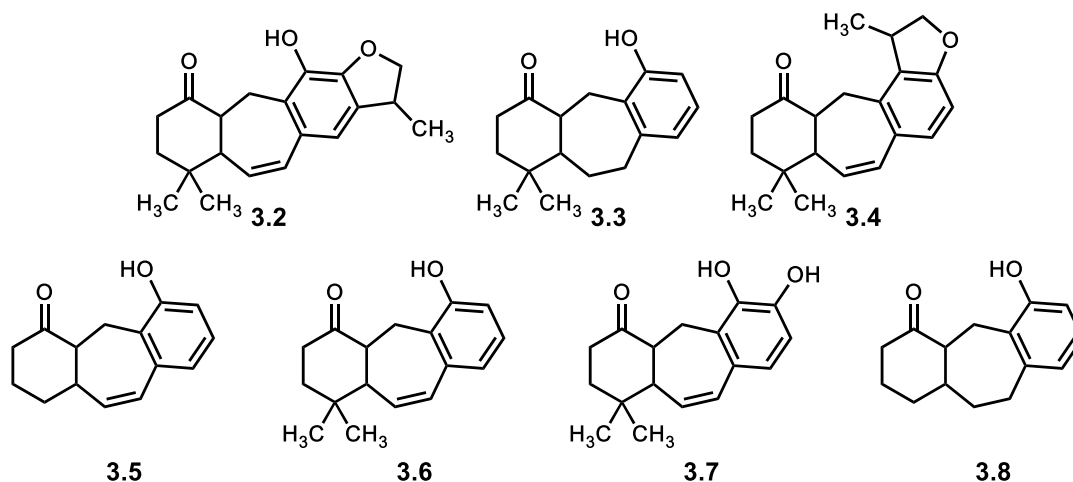


Figure 3.2 Previously synthesized icetexane analogues

My targets are analogues **3.9**, **3.10**, and **3.11**. In **3.10**, the impact of the saturation between C(6) and C(7) on biological activity can be compared to that of the presence of said unsaturation in **3.9**. Similarly, the impact of the absence of the gem-dimethyl at C(4) in **3.11** on biological activity can be compared to that of the presence of the C(4) gem-dimethyl **3.9**.

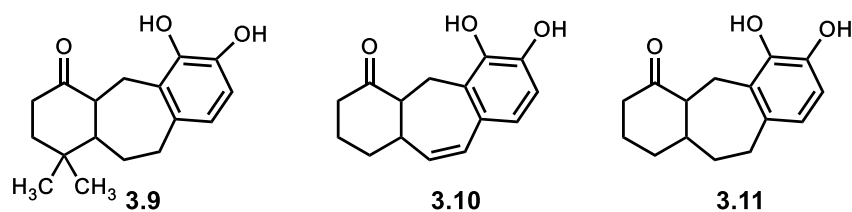


Figure 3.3 This work's targeted icetexane analogues

3.2 Synthesis of Analog 3.9

Continuing from Dr. Naeini and Ziegelmeier's works and following the precedent of the Moon paper, analogues were desired to probe a greater structure activity relationship of the less complex premmnatifolin A analogues. To this end, I pursued the syntheses of a range of different

analogues **3.9**, **3.10**, and **3.11**. These targets were chosen for their ease of synthesis and ability to probe chemical space and determine structure activity relationships of multiple functionalities on the analogues. The hydrogenated analog of **3.7** was desired to investigate the activity of the styrene unit.

First, the right-hand side **3.17** of the desired analog **3.9** was synthesized. Using published methods, methoxybenzaldehyde **3.13** was methylated from dihydroxybenzaldehyde **3.12** under the influence of base and methyl iodide in a 93% yield.⁵⁰ Sodium borohydride was then used to reduce dimethoxybenzaldehyde **3.13** to benzylic alcohol **3.14** with a 95% yield.⁵¹ Benzylic alcohol **3.14** was brominated under the action of N-Bromosuccinimide to **3.15** in 67% yield.⁵² The Suzuki-Miyaura cross coupling of **3.15** to **3.16** was attempted with a tetrakis(triphenylphosphine)palladium(0) catalyst using procedures from Naeini, but separation of the product **3.16** from the catalyst proved to be challenging and low yielding. After several failed attempts, the cross coupling was realized using alternative conditions with a palladium(II) acetate catalyst, giving **3.16** in 73% yield. **3.16** was then subjected to triethylamine and methanesulfonyl chloride to give intermediate **3.17** in 65% yield.

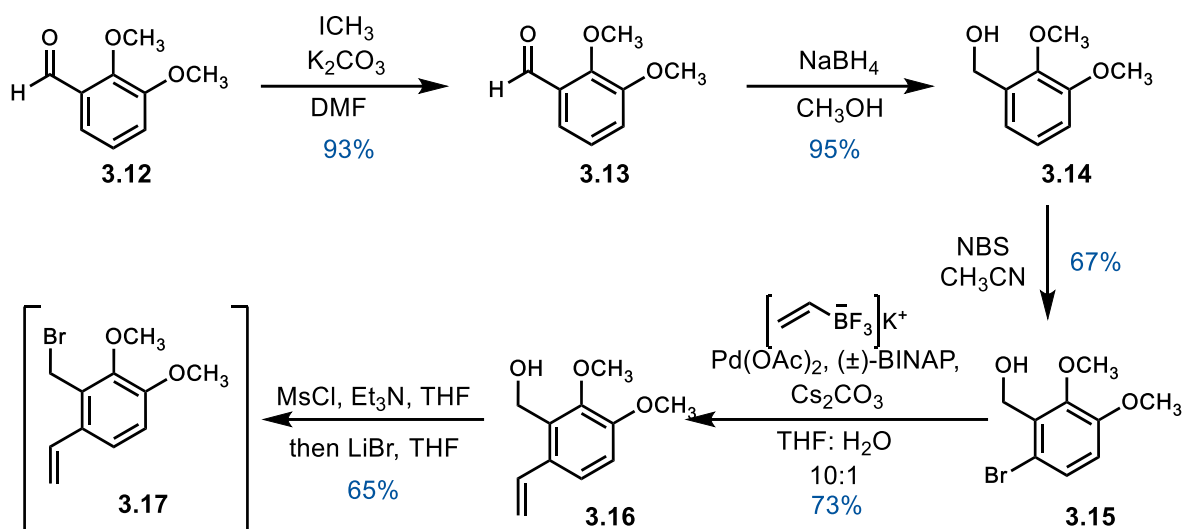


Figure 3.4 Synthetic route to the right-hand side **3.17** of analog **3.9**

The synthesis of the left-hand side, enolate **3.19** of analog **3.9** was much shorter and completed in a one pot two-step process. 4,4-dimethylcyclohexenone **3.18** was first treated with vinylmagnesium bromide and copper iodide at $-78\text{ }^\circ\text{C}$ before being treated with trimethylsilane chloride and triethylamine and allowed to warm to room temperature.^{10a} Using Ziegler's optimized alkylation conditions, enolate **3.19** and **3.17** were joined together under the action of tetramethylammonium fluoride, giving intermediate **3.20**. The ring-closing olefin metathesis strategy was employed to convert intermediate **3.20** into icetexane **3.21** under the action of the Grubbs 2nd generation catalyst. From bromide **3.17**, icetexane **3.21** was isolated in 54% yield over two steps. Icetexane **3.21** was then hydrogenated using hydrogen gas and palladium on carbon to yield analog **3.7** in 91% yield. Subsequent treatment of analog **3.7** with boron tribromide gave analog **3.9** in 59% yield. We currently await bioactivity results of analog **3.9** against the NCI-60 panel of 60 different model cancer cell lines.

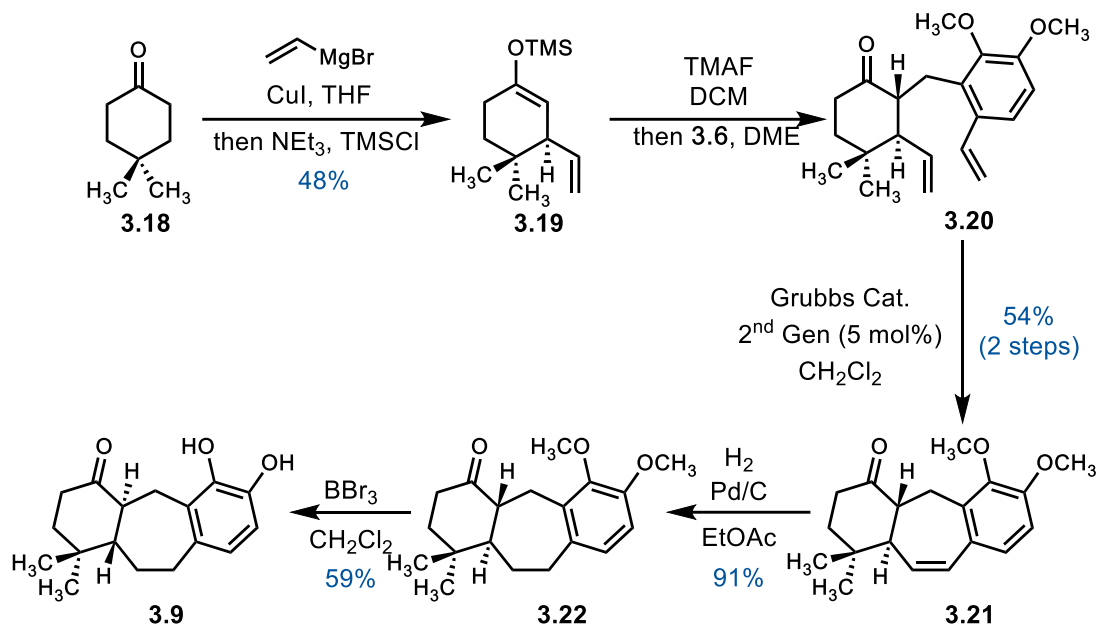


Figure 3.5 Synthetic route to analog **3.9**

3.3 Synthesis of Analogs **3.10** and **3.11**

The synthesis of analogues **3.10** and **3.11** proceeds similarly. The right-hand side **3.17** is built using the synthesis plan described above.

The synthesis of the left-hand side, enolate **3.24** was completed in a one pot two-step process similar to the aforementioned synthesis of analog **3.9**. Cyclohexenone **3.23** was first treated with vinylmagnesium bromide and copper iodide at $-78\text{ }^\circ\text{C}$ before being treated with trimethylsilane chloride and triethylamine and allowed to warm to room temperature. Silyl enol ether **3.24** and **3.17** were joined together under the action of tetramethylammonium fluoride, giving intermediate **3.25**. The ring-closing olefin metathesis strategy was employed to convert intermediate **3.25** into protected icetexane **3.26** under the action of the Grubbs 2nd generation catalyst. From silyl enol ether **3.24**, icetexane **3.26** was isolated in 31% yield over two steps. Icetexane **3.26** was then de-methylated under the action of boron tribromide to afford analog **3.10**

in 27% yield. We currently await bioactivity results of analog **3.10** against the NCI-60 panel of 60 different model cancer cell lines.

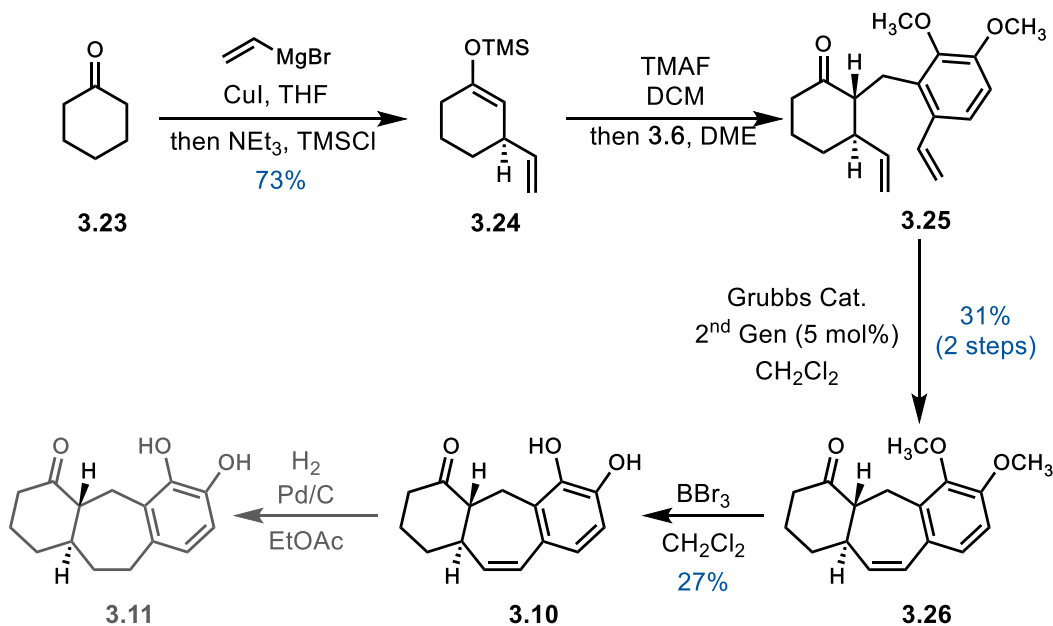


Figure 3.6 Synthetic route to analog **3.10**

Analog **3.10** was then hydrogenated under the action of palladium on carbon. Upon reduction we await purification by flash column chromatography to investigate the viability of this method and is currently where the project resides.

3.4 Summary

The need for a more efficient chemotherapeutic treatment against breast cancer and the exciting diversity in icetexanes motivated us to develop methods for the synthesis of different icetexanes. Inspired by the remarkable works of Dr. Ali Amiri Naeni and Mr. Alex Ziegelmeier in the Chain Laboratory, I worked to enlarge the library of synthesized icetexanes in Chain lab,

including **3.9**, **3.10**, and **3.11**. During this work, the synthesis of icetexanes **3.9** and **3.10** was completed, and we are poised to complete the synthesis of **3.11**. These icetexane analogues will be evaluated against a panel of human breast cancer cell lines and the NCI-60. Further synthesis of various icetexanes to identify new lead compounds for human cancer chemotherapeutic agents is also desirable.

References

1. Muluye, R. A.; Bian, Y.; Alemu, P. A. *J. Tradit. Complement Med.* **2014**, 4(2), 93–98.
2. Rezai, S.; Rahzani, K.; Hekmatpou, D.; Rostami, A. *Scars, Burns & Heal* **2023**, 9, 205951312211340.
3. Patridge, E.; Gareiss, P.; Kinch, M. S.; Hoyer, D. *Drug Discovery Today* **2016**, 21(2), 204–207.
4. Suresh, G.; Babu, K. S.; Rao, M. S. A.; Rao, V. R. S.; Yadav, P. A.; Nayak, V. L.; Ramakrishna, S. *Tetrahedron Lett.* **2011**, 52, 5016–5019.
5. a) Sato, T.; Hotsumi, M.; Makabe, K.; Kono, H. *Bioorg. Med. Chem. Lett.* **2018**, 28, 3520–3525; b) Detterbeck, R.; Hesse, M. *Helv. Chim. Acta* **2003**, 86, 343–360; c) McManus, H. A.; Fleming, M. J.; Lautens, M. *Angew. Chem.* **2007**, 119, 437–440; d) Qandil, A. M.; Ghosh, D.; Nicholas, D. E. *J. Org. Chem.* **1999**, 64, 1407–1409.
6. Watson, W. H.; Taira, Z.; Dominguez, X. A.; Gonzales, H.; Guitierrez, M.; Aragon, R. *Tetrahedron Lett.* **1976**, 17, 2501–2502.
7. El-Lakany, A. M.; Abdel-Kader, M. S.; Sabri, N. N.; Stermitz, F. R. *Planta Med.* **1995**, 61, 559–560.
8. Salae, A.-W.; Rodjun, A.; Karalai, C.; Ponglimanont, C.; Chantrapromma, S.; Kanjana-Opas, A.; Tewtrakul, S.; Fun, H.-K. *Tetrahedron* **2012**, 68, 819–829.
9. Uchiyama, N.; Kiuchi, F.; Ito, M.; Honda, G.; Takeda, Y.; Khodzhimatov, O.K.; Ashurmetov, O.A. *J. Nat. Prod.* **2003**, 66, 128–131.
10. a) Moon, D. J.; Al-Amin, M.; Lewis, R. S.; Arnold, K. M.; Yap, G. P. A.; Sims-Mourtada, J.; Chain, W. J. *Eur. J. Org. Chem.* **2018**, 25, 3348–3351. b) Naeini, A. A.; Ziegelmeier, A.

- A.; Chain, W. J. *Chemistry & Biodiversity* **2022**, 19(11). c) Simmons, E. M.; Sarpong, R. *Natural Product Reports*, **2009**, 26(9), 1195.
11. Miyase, T.; Ruedi, P.; Eugster, C. H. *Helv. Chim. Acta*, 1977, 60, 2789–2803.
12. Yatagai, M.; Takahashi, T. *Phytochemistry* **1980**, 19, 1149–1151.
13. Hasegawa, S.; Hirose, Y.; Yatagai, M.; Takahashi, T. *Chem. Lett.* 1984, **13**, 1837–1838.
14. Kelecom, A. *Tetrahedron* 1983, **39**, 3603–3608.
15. Liang, J. Y.; Min, Z. D.; Inuma, M.; Tanaka, T.; Mizuno, M. *Chem. Pharm. Bull.* 1987, **35**, 2613–2614.
16. Frontana, B.; Cárdenas, J.; Rodríguez-Hahn, L. *Phytochemistry* 1994, **36**, 739–741.
17. Hymavathi, A.; Babu, K. S.; Naidu, V. G.; Krishna, S. R.; Diwan, P. V.; Rao, J. M. *Bioorg. Med. Chem. Lett.* 2009, **19**, 5727–5731.
18. Sanchez, C.; Cardenas, J.; Rodriguez–Hahn, L.; Ramamoorthy, T. P. *Phytochemistry* **1989**, 28, 1681–1684.
19. Gonzalez, A. G.; Andres, L. S.; Luis, J. G.; Brito, I.; Rodriguez, M. L. *Phytochemistry* **1991**, 30, 4067–4070.
20. Fraga, B. M.; Diaz, C. E.; Guadano, A.; Gonzalez–Coloma, A. J. *Agric. Food Chem.* **2005**, 53, 5200–5206.
21. Matsumoto, T.; Imai, S.; Yoshinari, T.; Matsuno, S. *Bull. Chem. Soc. Jpn.* 1986, **59**, 3103–3108.
22. (a) Matsumoto, T.; Usui, S. *Bull. Chem. Soc. Jpn.* 1979, **52**, 212–215. (b) Schöllkopf, U. *Angew. Chem.* 1959, **71**, 260–273.
23. Crandall, J.; Apparau, M. *Org. React.* 1983, **29**, 345–443.

24. (a) Majetich, G.; Li, Y.; Zou, G. *Heterocycles* 2007, **73**, 227–235. (b) Majetich, G.; Yu, J.; Li, Y. *Heterocycles* 2007, **73**, 217–225.
25. Isler, O.; Montavon, M.; Rüegg, R.; Zeller, P. *Helv. Chim. Acta.* 1956, **39**, 259–273.
26. Stork, G.; Danheiser, R. L. *J. Org. Chem.* 2002, **38**, 1775–1776.
27. Lindlar, H. *Helv. Chim. Acta.* 1952, **35**, 446–450.
28. Corey, E. J.; Bakshi, R. K.; Shibata, S. *J. Am. Chem. Soc.* 1987, **109**, 5551–5553.
29. Myers, A. G.; Zheng, B. *Tetrahedron Lett.* 1996, **37**, 4841–4844.
30. Munir, A. A. *Adelaide Bot Gard.* **1984**; 7:1–44.
31. Ruwali, P.; Negi, D. *J. Pharm. Innov.* **2019**, 8(5), 13–20.
32. Chopra, R. N., Nayar, S.L., Chopra, I.C. Glossary of Indian Medicinal Plant, (CSIR Publications, New Delhi), 1992, 203.
33. (a) Kalaichelvi, K.; Dhivya, S. M. *J Med. Plants Studies.* **2016**; 4(4):84-87. (b) Nadkarni, A. K. Indian material medica. New Delhi: Popular Prakashan, 1985, 1008.
34. Suresh, G.; Babu, K. S.; Rao, V. R. S.; Rao, M. S. A.; Nayak, V. L.; Ramakrishna, S. *Tetrahedron Lett.* **2011**, 52, 1273–1276.
35. Chatterjee, K.; Zhang, J.; Honbo, N.; Karliner, J. S. *Cardiology* **2010**, 115, 115–162.
36. (a) Chen, Y.; Huang, J.; Liu, B. *Tetrahedron Lett.*, 2010, **51**, 4655. (b) Jones, T. K.; Denmark, S. E. *J. Org. Chem.*, 1985, **50**, 4037. (c) Bergmann, E. D.; Ginsburg D.; Pappo, R. *Org. React.*, 1959, **10**, 179. (d) Little, R. D.; Masjedizadeh, M.R.; Wallquist, O.; McLoughlin, J. I. *Org. React.*, 1995, **47**, 316.
37. (a) Anelli, P. L.; Banfi, S.; Legramandi, F.; Montanari, F.; Pozzi, G.; Quici, S. *J. Chem. Soc., Perkin Trans. 1*, **1993**, 1345. (b) Vilain, S.; Maillard, P.; Momenteau, M. *J. Chem. Soc., Chem. Commun.*, **1994**, 1697.

38. (a) Alacid, E.; Nájera, C. *J. Org. Chem.*, 2009, **74**, 8191. (b) Birkholz, M. -N.; Freixa, Z.; van Leeuwen, P. *Chem. Soc. Rev.*, 2009, **38**, 1099. (c) Molander, G. A.; Brown, A. R. *J. Org. Chem.*, 2006, **71**, 9681.
39. Lewis, R. S.; Garza, C. J.; Dang, A. T.; Pedro T. -K. A.; Chain, W. J. *Org. Lett.*, 2015, **17**, 2278.
40. Grubbs, R. H.; Chang, S. *Tetrahedron*, 1998, **54**, 4413.
41. (a) Sato, T.; Hotsumi, M.; Makabe, K.; Kono, H. *Bioorg. Med. Chem. Lett.* **2018**, 28, 3520–3525; (b) Detterbeck, R.; Hesse, M. *Helv. Chim. Acta* **2003**, 86, 343–360; (c) McManus, H. A.; Fleming, M. J.; Lautens, M. *Angew. Chem.* **2007**, 119, 437–440; (d) Qandil, A. M.; Ghosh, D.; Nicholas, D. E. *J. Org. Chem.* **1999**, 64, 1407–1409.
42. (a) Molander, G. A.; Rivero, M. R. *Org. Lett.* **2002**, 4, 107–109; (b) Alacid, E.; Najera, C. *J. Org. Chem.* **2009**, 74, 8191–8195.
43. Dixon, D. D.; Sethumadhavan, D.; Benncehe, T.; Banaag, A. R.; Tius, M. A.; Thakur, G. A.; Bowman, A.; Wood, J. T.; Makriyannis, A. J. *Med. Chem.* **2010**, 53, 5656–5666.
44. Grubbs, R. H.; Vougioukalakis, G. C. *Chem. Rev.* **2010**, 110, 1746–1787.
45. (a) Garcia, O.; Nicolas, E.; Albericio, F. *Tetrahedron Lett.* **2003**, 44, 4961–4963. (b) Vilsmeier, A.; Haack, A. *Ber. Dtsch. Chem. (A and B Series)* **1927**, 60, 119–122; (c) Barluenga, J.; Campos, P. J.; Gonzalez–Nuñez, E.; Asensio, G. *Synthesis* **1985**, 1985, 426–428.
46. Pearl, I. A. *Org. Synth.* **1950**, 30, 101.
47. Fu, J.; Lundy, W.; Chowdhury, R.; Twitty, J. C.; Dinh, L. P.; Sampson, J.; Lam, Y. -H.; Sevov, C. S.; Watson, M. P.; Kalyani, D. *ACS Catal.* **2023**, 13, 14, 9336–9345.

48. Munawar, S.; Zahoor, A. F.; Ali, S.; Javed, S.; Irfan, M.; Irfan, A.; Kotwica-Mojzych, K.; Mojzych, M. *Molecules*. **2022**, 27(20), 6953.
49. Liu, S.; Trauner, D. *J. Am. Chem. Soc.* **2017**, 139, 9491–9494.
50. Sato, T.; Hotsumi, M.; Makabe, K.; Konno, H. *Bioorg. Med. Chem. Lett.* **2018**, 28, 3520–3525.
51. D., Subhadip; C., Saikat; M., Sourabh; M., Himanshu; B., Alakesh. *J. Ind. Chem. Soc.* **2013**, 90, 1871–1884.
52. Schmidt, E. A.; Hoffmann, H. M. R. *J. Am. Chem. Soc.* **1972**, 94, 7832–7837.

Experimental Procedures

General Information: *These experimental procedures have been published previously in its current or a substantially similar form and I have obtained permission to republish it.*¹

Proton (¹H), carbon (¹³C), fluorine (¹⁹F), and silicon (²⁹Si) nuclear magnetic resonance (NMR) spectra were recorded on Bruker AV400 CryoPlatform QNP or Bruker AVIII600 SMART NMR spectrometers at 23 °C. Proton chemical shifts are expressed in parts per million (ppm, δ scale) downfield from tetramethylsilane and are referenced to residual protium in the NMR solvent (CHCl₃: δ 7.26, C₆D₆: δ 7.16). Carbon chemical shifts are expressed in parts per million (ppm, δ scale) downfield from tetramethylsilane and are referenced to the carbon resonance of the NMR solvent (CDCl₃: δ 77.16, C₆D₆: δ 128.06). Data are represented as follows: chemical shift, multiplicity (s = singlet, d = doublet, t = triplet, q = quartet, m = multiplet, br = broad, app = apparent), integration, and coupling constant (*J*) in Hertz (Hz). High-resolution mass spectra were obtained using an Agilent 1100 quaternary LC system coupled to an Agilent 6210 LC/MSD-TOF fitted with an ESI or an APCI source, or Thermo Q-Exactive Orbitrap using electrospray ionization (ESI) or a Waters GCT Premier spectrometer using chemical ionization (CI). Unless otherwise noted, column chromatography was performed either manually or by use of a Biotage Isolera One unit with 40–63 μ m silica gel, and the eluent reported in parentheses. Analytical thin-layer chromatography (TLC) was performed using glass plates pre-coated with silica gel (0.25 mm, 60-Å pore size, 5–20 μ m, Silicycle) impregnated with a fluorescent indicator (254 nm). TLC plates were visualized by exposure to ultraviolet light (UV), then were stained by immersion in iodine-impregnated silica gel, submersion in aqueous ceric ammonium molybdate solution (CAM), ethanolic phosphomolybdic acid solution (PMA), acidic ethanolic p-anisaldehyde solution

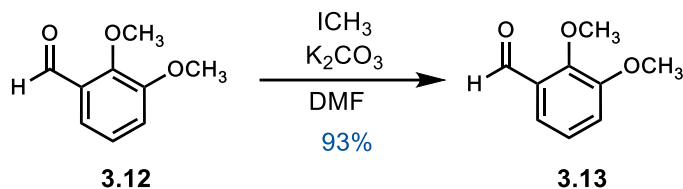
¹ Naeini, A. A. Ph.D. Dissertation, University of Delaware, Newark, DE, 2022.

(anisaldehyde), aqueous ceric phosphomolybdic solution (“Magic”)¹, or aqueous potassium permanganate solution (KMnO₄), followed by brief heating on a hot plate (215 °C, 10–15 s).

Materials: Commercial reagents and solvents were used as received with the following exceptions. Triethylamine, dichloromethane, diethyl ether, tetrahydrofuran, dimethylsulfoxide, toluene, benzene, *N,N*-dimethylformamide, and 1,2-dimethoxyethane were purified by the method of Pangborn, et al.² All reactions were performed in a single-neck oven- or flame-dried round bottom flasks fitted with rubber septa under a positive pressure of argon, unless otherwise noted. Air- and moisture-sensitive liquids were transferred via syringe or stainless-steel cannula. All temperatures reported are external readings of the oil bath heating the reaction vessel. Organic solutions were concentrated by rotary evaporation at or below 35 °C at 10 Torr (diaphragm vacuum pump) unless otherwise noted.

² Pangborn, A. B.; Giardello, M. A.; Grubbs, R. H.; Rosen, R. K.; Timmers, F. J. *Organometallics* **1996**, 15, 1518–1520.

Synthesis of Methoxybenzaldehyde 3.13³



Iodomethane (2.03 mL, 32.6 mmol, 2.25 equiv) was added to a stirred suspension of 2,3-dihydroxybenzaldehyde (2.00g, 14.5 mmol, 1.00 equiv) and potassium carbonate (4.50g, 32.6 mmol, 2.25 equiv) in *N,N*-dimethylformamide (145 mL) and the resultant yellow mixture was stirred at 80 °C for 2h. The resultant solution was then cooled to 23 °C and diluted with water (150mL). The resultant mixture was then extracted with diethyl ether (5 x 150 mL). The combined organic layers were washed with saturated aqueous sodium chloride solution (50 mL), dried over anhydrous sodium sulfate, and the dried solution was concentrated. The residue was diluted with diethyl ether (150 mL) and washed with 2.0 M aqueous lithium chloride solution (3 x 150 mL) and saturated aqueous sodium chloride solution (50 mL). The combined organic layers were dried over anhydrous sodium sulfate and the dried solution was concentrated to afford 2,3-dimethoxybenzaldehyde **3.13** as a yellow solid (2.24 g, 13.5 mmol, 93%).

¹H NMR (400 MHz, CDCl₃), δ: 10.44 (s, 1H), 7.44 – 7.40 (m, 1H), 7.17 – 7.11 (m, 2H), 3.99 (s, 3H), 3.91 (s, 3H).

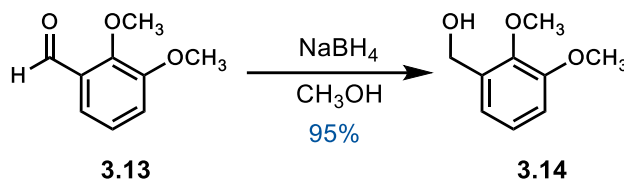
¹³C NMR (100 MHz, CDCl₃), δ: 190.6, 153.4, 153.1, 130.2, 124.6, 119.6, 118.5, 77.8, 77.5, 77.2, 62.9, 56.5.

TLC: 20% ethyl acetate–hexanes, R_f = 0.39

³ Sato, T.; Hotsumi, M.; Makabe, K.; Konno, H. *Bioorg. Med. Chem. Lett.* **2018**, 28, 3520–3525.

(UV, CAM).

Synthesis of Benzylic Alcohol 3.14⁴



Sodium borohydride (0.31 g, 8.08 mmol, 0.60 equiv) was added in portions to a stirred solution of 2,3–methoxybenzaldehyde (2.24 g, 13.47 mmol, 1.00 equiv) in methanol (7.9 mL) at 23 °C. The resultant solution was stirred at 23 °C for 1 h, then was concentrated. The resulting yellow oil was diluted with water (20 mL) and extracted with dichloromethane (4 x 30mL) until no product remained in the aqueous layer (TLC analysis). The combined organic layers were washed with saturated aqueous sodium chloride solution (30 mL) and then were dried over anhydrous sodium sulfate. The dried solution was concentrated to afford 2,3–dihydroxybenzyl alcohol **3.14** (2.15 g, 12.8 mmol, 95%) as a pale-yellow oil.

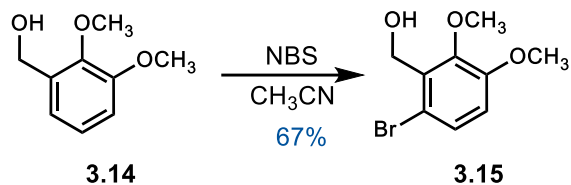
¹H NMR (400 MHz, CDCl₃), δ: 7.05 (t, *J* = 7.9 Hz, 1H), 6.93 (dd, *J*₁ = 7.8 Hz, *J*₂ = 1.5 Hz, 1H), 6.89 (dd, *J*₁ = 8.2 Hz, *J*₂ = 1.5 Hz, 1H), 4.70 (s, 2H), 3.88 (d, *J* = 11.2 Hz, 6H).

¹³C NMR (100 MHz, CDCl₃), δ: 152.5, 147.1, 134.6, 124.2, 120.7, 112.3, 61.7, 60.9, 55.8.

TLC: 20% ethyl acetate–hexanes, *R*_f = 0.15 (UV, CAM).

⁴ D., Subhadip; C., Saikat; M., Sourabh; M., Himanshu; B., Alakesh. *J. Ind. Chem. Soc.* **2013**, 90, 1871–1884.

Synthesis of 3.15⁵



N-Bromosuccinimide (2.73 g, 15.4 mmol, 1.20 equiv) was added in one portion to a stirred solution of **3.3** (2.15 g, 12.8 mmol, 1.00 equiv) in acetonitrile (9.6 mL) at 23 °C. The resultant mixture was stirred for 30 min at which point the *N*-bromosuccinimide was fully dissolved. The resulting solution was then diluted with diethyl ether (25 mL) and filtered. The filtrate was washed sequentially with 2.0 M aqueous sodium hydroxide solution (2 x 25 mL) and saturated aqueous sodium chloride solution (15 mL). The resultant organic layer was dried over anhydrous sodium sulfate and the dried solution was concentrated. The resultant oily residue was purified by flash column chromatography (silica gel, 20% ethyl acetate–hexanes) to afford **3.15** (2.12 g, 8.57 mmol, 67%) as a yellow oil.

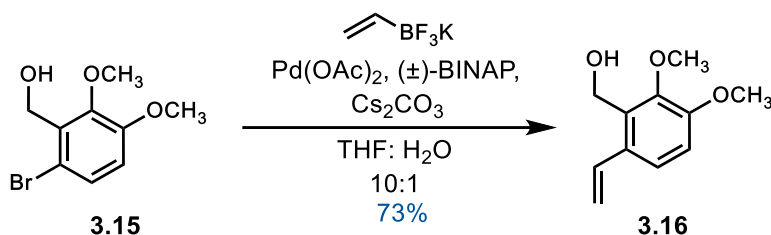
¹H NMR (400 MHz, CDCl₃), δ: 7.27 (d, *J* = 8.8 Hz, 1H), 6.77 (d, *J* = 8.8 Hz, 1H), 4.83 (s, 2H), 3.90 (s, 3H), 3.85 (s, 3H), 152.7, 149.1, 134.2, 128.3, 115.2, 113.7, 62.1,

¹³C NMR (100 MHz, CDCl₃), δ: 60.7, 56.4.

TLC: 20% ethyl acetate–hexanes, *R_f* = 0.15
(UV, CAM).

⁵ Schmidt, E. A.; Hoffmann, H. M. R. *J. Am. Chem. Soc.* **1972**, *94*, 7832–7837.

Synthesis of 3.16



Cesium carbonate (8.38 g, 25.7 mmol, 3.00 equiv) was added to a stirred solution of **3.4** (2.12 g, 8.57 mmol, 1.0 equiv), potassium vinyltrifluoroborate (2.00 g, 14.9 mmol, 1.74 equiv), palladium(II) acetate (0.19 g, 0.86 mmol, 0.10 equiv) and 2,2'-bis(diphenylphosphino)-1,1'-binaphthyl (1.07 g, 1.71 mmol, 0.20 equiv) in tetrahydrofuran : water (56 mL : 5.6 mL) in a glass pressure reactor. The deep red mixture was sparged with argon for 15 min at which point the solution turned yellow and was sealed under an atmosphere of argon and stirred at 85 °C for 24h. The resultant mixture was cooled to 23 °C and quenched by the addition of water (160 mL). The resultant mixture was extracted with diethyl ether (3 x 150 mL). The combined organic layers were washed with saturated aqueous sodium chloride solution (100 mL) and then dried over anhydrous sodium sulfate. The dried solution was concentrated, and the residue was purified by flash column chromatography (silica gel, 20% ethyl acetate–hexanes) to afford a **3.16** (1.22 g, 6.26 mmol, 73%) as a yellow-orange oil.

^1H NMR (400 MHz, CDCl_3), δ : 7.25 (d, $J = 9.8$ Hz, 3H), 7.01 (dd, $J_1 = 17.3$, $J_2 = 10.9$ Hz, 1H), 6.88 (d, $J = 8.6$ Hz, 1H), 5.58 (dd, $J_1 = 17.3$, $J_2 = 1.4$ Hz, 1H), 5.28 (dd, $J_1 = 10.9$, $J_2 = 1.4$ Hz, 1H), 4.79 (d, $J = 6.2$ Hz,

2H), 3.91 – 3.85 (m, 6H), 1.98 (t, $J = 6.2$ Hz, 1H).

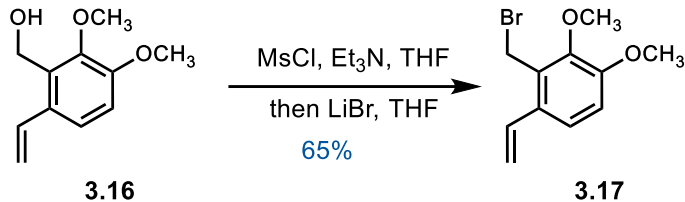
^{13}C NMR (100 MHz, CDCl_3), δ : 152.5, 147.8, 134.1, 132.1, 131.2, 122.5, 115.9, 112.6, 61.7, 57.3, 56.2.

FTIR (KBr, thin film), cm^{-1} : 3418, 2940, 1624

HRMS ES^+ $[\text{M}+\text{H}]^+$: Calcd for $\text{C}_{11}\text{H}_{15}\text{O}_3$: 195.01016. Found: 195.1013.

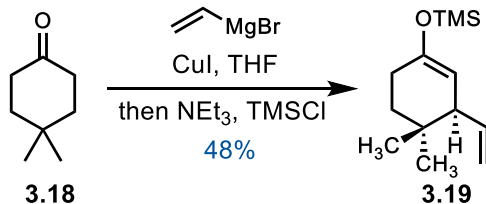
TLC: 20% ethyl acetate–hexanes, $R_f = 0.17$
(UV, CAM, anisaldehyde).

Synthesis of 3.17



A solution of **3.5** (250 mg, 1.29 mmol, 1.00 equiv) in tetrahydrofuran (16.7 mL) was cooled to $-40\text{ }^{\circ}\text{C}$. Triethylamine (1.2 mL, 8.39 mmol, 6.52 equiv) and methanesulfonyl chloride (0.6 mL, 8.30 mmol, 6.45 equiv) were added sequentially and the resultant solution was stirred for 50 min. The solution was then warmed to $0\text{ }^{\circ}\text{C}$ and stirred for 30 min. Flame-dried lithium bromide (1.11 g, 12.8 mmol, 9.92 equiv) in tetrahydrofuran (7.6 mL) was added via cannula and the resultant solution was stirred for an additional 10 min at $0\text{ }^{\circ}\text{C}$. The reaction mixture was then allowed to warm to $23\text{ }^{\circ}\text{C}$ and stirred for 40 min before it was cooled to $0\text{ }^{\circ}\text{C}$ and quenched with sodium bicarbonate (20 mL). The resultant mixture was extracted with ethyl acetate (3 x 25 mL). The combined organic layers were washed with saturated aqueous sodium chloride solution (30 mL) and then dried over anhydrous sodium sulfate. The dried solution was concentrated and purified through a short column of basic alumina to afford **3.17** (217 mg, 0.84 mmol, 65%) as a yellow oil.

Synthesis of **3.19**⁶



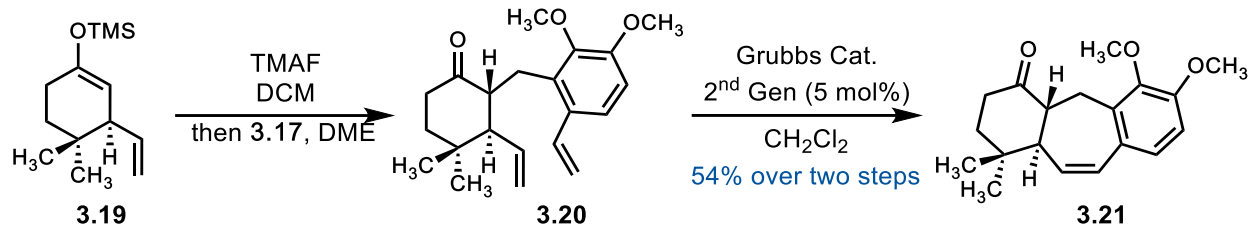
Vinylmagnesium bromide (1.0 M in tetrahydrofuran, 9.1 mL, 9.1 mmol, 2.39 equiv) was added to stirred solution of copper iodide (860 mg, 4.55 mmol, 1.20 equiv) in tetrahydrofuran (15 mL) cooled to $-78\text{ }^{\circ}\text{C}$. The resultant mixture was stirred for 15 min at which point 4,4-Dimethylcyclohexanone **3.7** (0.5 mL, 3.80 mmol, 1.00 equiv) was added in one portion and the resultant solution was stirred for 1 h. At which point triethylamine (1.6 mL, 11.4 mmol, 3.00 equiv) and chlorotrimethylsilane (1.5 mL, 12.2 mmol, 3.20 equiv) were added sequentially to the mixture and the resultant solution was allowed to warm to $23\text{ }^{\circ}\text{C}$ and stirred for an additional 3 h. The reaction was then quenched with saturated aqueous 9:1 $\text{NH}_4\text{Cl}:\text{NH}_4\text{OH}$ solution (25 mL) and the resultant mixture was extracted with diethyl ether (30 mL). The resultant organic layer was washed with saturated aqueous 9:1 $\text{NH}_4\text{Cl}:\text{NH}_4\text{OH}$ solution (30 mL) until the organic layer no longer appeared blue. The combined organic layers were washed with aqueous sodium chloride and dried with anhydrous sodium sulfate. The dried solution was then concentrated. The concentrated residue was purified by flash column chromatography (deactivated silica gel, pentane) to afford ((4,4-dimethyl-3-vinylcyclohex-1-en-1-yl)oxy)trimethylsilane **3.19** as a yellow oil (408 mg, 2.18 mmol, 48%).

⁶ Moon, D. J.; Al - Amin, M.; Lewis, R. S.; Arnold, K. M.; Yap, G. P. A.; Sims - Mourtada, J.; Chain, W. J. *Eur. J. Org. Chem.* **2018**, 25, 3348–3351.

^1H NMR (600 MHz, CDCl_3) δ : 5.75 – 5.68 (m, 1H), 5.02 – 4.96 (m, 2H), 4.68 – 4.65 (m, 1H), 2.06 – 1.94 (m, 2H), 1.51 – 1.44 (m, 1H), 1.37 (dt, $J = 13.5, 7.0$ Hz, 1H), 0.95 (s, 3H), 0.79 (s, 3H), 0.19 (d, $J = 1.2$ Hz, 9H).

^{13}C NMR (151 MHz, CDCl_3) δ : 150.3, 140.6, 115.3, 107.0, 50.1, 35.4, 31.8, 28.3, 27.9, 23.7, 0.3.

Synthesis of 3.21



A solution of ((4,4-dimethyl-3-vinylcyclohex-1-en-1-yl)oxy)trimethylsilane **3.19** (381 mg, 1.70 mmol, 2.01 equiv) in dichloromethane (5.5 mL) was added via cannula transfer to a 50 mL round bottom flask cooled to $-78\text{ }^{\circ}\text{C}$ with tetramethylammonium fluoride (165 mg, 1.77 mmol, 2.10 equiv). The resultant orange-brown solution was stirred for 5 min at which point **3.17** (217 mg, 0.844 mmol, 1.00 equiv.) in dichloromethane (2.7 mL) was added via cannula to the reaction mixture. The resultant opaque orange reaction mixture was allowed to warm to $23\text{ }^{\circ}\text{C}$ and stirred for 24 h. The reaction mixture was quenched with water (10 mL) and the resultant mixture was extracted with dichloromethane (3 x 15 mL). The combined organic layers were washed with saturated aqueous sodium chloride solution (10 mL), dried over anhydrous sodium sulfate, and the dried solution was concentrated. The resultant yellow oily concentrate was purified by flash column chromatography (silica gel, 5% ethyl acetate–hexanes) to afford crude **3.20** (213 mg) as a black–yellow oil. Grubbs second-generation catalyst (28 mg, 0.03 mmol, 0.05 equiv) was added to a stirred solution of **3.20** (213 mg) in dichloromethane (13 mL) at $23\text{ }^{\circ}\text{C}$. The resultant red solution was heated at $65\text{ }^{\circ}\text{C}$ for 48 h, then cooled to $23\text{ }^{\circ}\text{C}$ and concentrated. The resultant black oily residue was purified by flash column chromatography (silica gel, 5% ethyl acetate–hexanes) to afford **3.21** (137 mg, 0.447 mmol, 54% over 2 steps) as a white solid.

$^1\text{H NMR}$ (600 MHz, CDCl_3) δ : 6.88 (d, $J = 8.4$ Hz, 1H), 6.72 (d, $J = 8.4$ Hz, 1H), 6.46 (d, $J = 12.5$ Hz, 1H), 5.75 (dd, $J_1 =$

12.6, $J_2 = 3.5$ Hz, 1H), 4.07 (d, $J = 14.8$ Hz, 1H), 3.85 (s, 3H), 3.77 (s, 3H), 2.58 (dd, $J_1 = 12.8$, $J_2 = 7.4$ Hz, 1H), 2.45 (dt, $J_1 = 16.2$, $J_2 = 8.9$ Hz, 1H), 2.36 (dt, $J_1 = 14.3$, $J_2 = 4.0$ Hz, 1H), 2.27 (dd, $J_1 = 14.6$, $J_2 = 7.9$ Hz, 1H), 1.76 – 1.69 (m, 2H), 1.13 (s, 3H), 1.02 (s, 3H).

^{13}C NMR (151 MHz, CDCl_3) δ :

211.0, 152.4, 146.3, 134.6, 130.7, 129.9, 129.6, 126.5, 109.8, 61.5, 58.0, 56.1, 51.3, 41.5, 38.8, 35.1, 30.0, 23.9, 20.3.

FTIR (KBr, thin film), cm^{-1} :

2959, 1713, 1596.

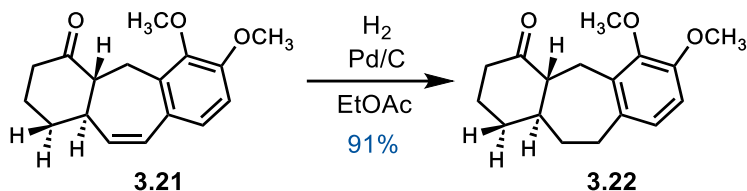
HRMS LIFDI⁺ [M]⁺:

Calcd for $\text{C}_{19}\text{H}_{24}\text{O}_3$: 300.1725. Found: 300.1730.

TLC:

20% ethyl acetate–hexanes, $R_f = 0.38$ (UV, CAM).

Synthesis of 3.22



Palladium on carbon (15 mg, 0.014 mmol, 0.1 equiv) was added to a 10mL round bottom flask and the sides of the flask were washed with ethyl acetate (0.6 mL). **3.21** (50 mg, 0.14 mmol, 1.0 equiv) in ethyl acetate (1 mL) was then added. The resultant slurry was placed under positive hydrogen pressure and stirred for 4 h. The resulting slurry was poured over a 1 cm silica plug and flushed with ethyl acetate (50 mL). The resultant solution was then concentrated to afford a **3.22** (38 mg, 0.13 mmol, 91%) as a yellow oil.

¹H NMR (600 MHz, CDCl₃) δ: 6.78 (d, *J* = 8.1 Hz, 1H), 6.65 (d, *J* = 8.2 Hz, 1H), 4.01 (d, *J* = 14.0 Hz, 1H), 3.82 (s, 3H), 3.74 (s, 3H), 2.75 – 2.67 (m, 2H), 2.52 (td, *J*₁ = 13.8, *J*₂ = 6.3 Hz, 1H), 2.36 – 2.31 (m, 1H), 2.23 – 2.14 (m, 2H), 1.76 – 1.65 (m, 2H), 1.61 (td, *J*₁ = 11.4, *J*₂ = 3.1 Hz, 1H), 1.27 – 1.18 (m, 2H), 1.01 (s, 3H), 0.97 (s, 3H).

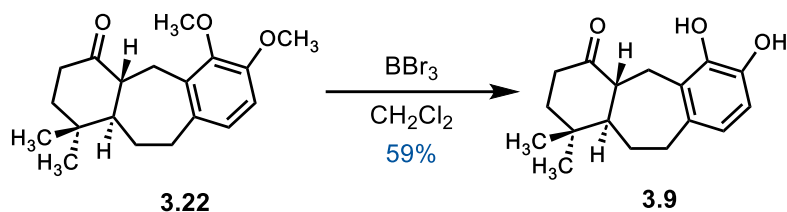
¹³C NMR (151 MHz, CDCl₃) δ: 212.5, 151.5, 147.1, 137.7, 134.6, 123.1, 109.8, 61.5, 58.2, 56.1, 51.1, 42.8, 38.7, 34.4, 34.3, 30.0, 29.8, 24.9, 20.4.

TLC:

20% ethyl acetate–hexanes, $R_f = 0.31$

(UV, DNP).

Synthesis of 3.9



Boron tribromide (1.0 M in dichloromethane, 0.22 mL, 0.22 mmol, 1.69 equiv) was added to a solution of **3.22** (38 mg, 0.13 mmol, 1.0 equiv) in dichloromethane (0.9 mL) cooled to $-40\text{ }^{\circ}\text{C}$. The resulting red orange solution was stirred for 2 h at $-40\text{ }^{\circ}\text{C}$. The reaction mixture was quenched with water (5 mL) and the resulting mixture was extracted with dichloromethane (3 x 10 mL). The combined organic layers were washed with saturated aqueous sodium chloride solution (10 mL), dried over anhydrous sodium sulfate, and the dried solution was concentrated. The resultant residue was purified twice by flash column chromatography (silica gel, 20% ethyl acetate–hexanes) to afford **3.9** (20 mg, 0.074 mmol, 59%) as a white solid.

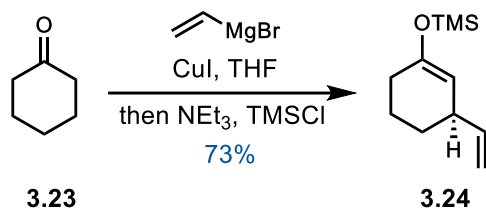
^1H NMR (600 MHz, CDCl_3) δ :

8.07 (s, 1H), 6.79 (d, $J = 8.1$ Hz, 1H), 6.65 – 6.60 (m, 2H), 5.92 (dd, $J_1 = 10.3$, $J_2 = 6.1$ Hz, 1H), 5.77 (s, 1H), 3.38 – 3.33 (m, 1H), 3.08 (d, $J = 14.0$ Hz, 1H), 2.55 (tdd, $J_1 = 13.9$, $J_2 = 6.7$, $J_3 = 1.3$ Hz, 1H), 2.36 – 2.31 (m, 2H), 1.90 – 1.86 (m, 1H), 1.77 (ddd, $J_1 = 13.7$, $J_2 = 6.7$, $J_3 = 2.4$ Hz, 1H), 1.54 – 1.49 (m, 1H), 1.26 (s, 3H), 0.90 (s, 3H).

^{13}C NMR (151 MHz, CDCl_3) δ :

216.9, 145.2, 141.4, 132.0, 131.4, 129.6, 126.0, 121.0, 112.6, 60.5, 52.0, 41.9, 38.5, 33.0, 29.5, 24.8, 20.2.

Synthesis of 3.24⁷



Vinylmagnesium bromide (1M in tetrahydrofuran, 12.5 mL, 12.5 mmol, 2.40 equiv) was added to stirred solution of copper iodide (1.19 g, 6.20 mmol, 1.20 equiv) in tetrahydrofuran (15 mL) cooled to $-78\text{ }^{\circ}\text{C}$. The resultant mixture was stirred for 15 min at which point cyclohexanone (0.5 mL, 5.20 mmol, 1.00 equiv) was added and the resultant solution stirred for 1 h at which point Triethylamine (2.2 mL, 15.6 mmol, 3.00 equiv) and trimethylsilyl chloride (3.0 mL, 15.6 mmol, 3.00 equiv) were added sequentially. The resultant solution was allowed to warm to $23\text{ }^{\circ}\text{C}$ and stirred for an additional 3 h. The reaction was then quenched with 9:1 $\text{NH}_4\text{Cl}:\text{NH}_4\text{OH}$ (25 mL) and the resultant mixture was extracted with diethyl ether (30 mL). The resultant organic layer was washed with saturated aqueous 9:1 $\text{NH}_4\text{Cl}:\text{NH}_4\text{OH}$ solution (30 mL) until the organic layer no longer appeared blue. The combined organic layers were washed with saturated aqueous sodium chloride solution, dried with anhydrous sodium sulfate, and the dried solution was concentrated. The concentrated residue was purified by flash column chromatography (deactivated silica gel, pentane) to afford (3-vinylcyclohex-1-en-1-yl)oxy)trimethylsilane **3.24** as a yellow oil (745 mg, 3.79 mmol, 73%).

^1H NMR (600 MHz, CDCl_3) δ : 5.80 – 5.74 (m, 1H), 5.01 – 4.93 (m, 2H), 4.77

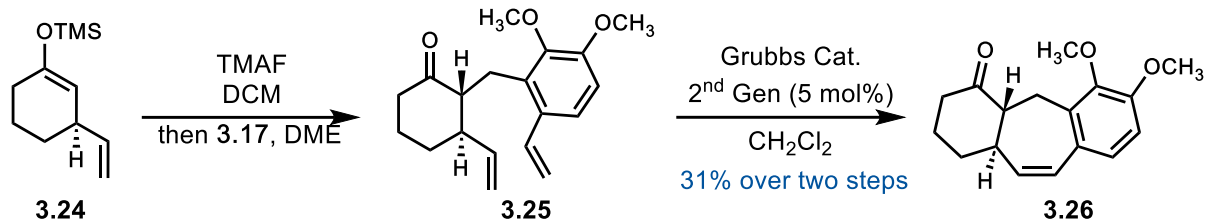
⁷ Moon, D. J.; Al - Amin, M.; Lewis, R. S.; Arnold, K. M.; Yap, G. P. A.; Sims - Mourtada, J.; Chain, W. J. *Eur. J. Org. Chem.* **2018**, 25, 3348–3351.

(dt, $J_1 = 3.1$, $J_2 = 1.4$ Hz, 1H), 2.01 – 1.96 (m, 2H), 1.76 – 1.68 (m, 2H), 1.61 – 1.54 (m, 2H), 1.33 – 1.26 (m, 1H), 0.19 (s, 9H).

^{13}C NMR (151 MHz, CDCl_3) δ :

151.6, 143.7, 113.4, 107.1, 39.1, 30.2, 29.1, 21.2, 0.7.

Synthesis of 3.26



A solution of ((4,4-dimethyl-3-vinylcyclohex-1-en-1-yl)oxy)trimethylsilane **3.24** (380 mg, 1.94 mmol, 2.01 equiv) in dichloromethane (6.2 mL) was added to the precooled ($-78\text{ }^{\circ}\text{C}$) flask containing tetramethylammonium fluoride (189 mg, 2.02 mmol, 2.10 equiv). The resultant orange-brown solution was stirred for 5 min at which point **3.17** (248 mg, 0.965 mmol, 1.0 equiv.) in dichloromethane (3.1 mL) was added via cannula. The resultant opaque orange solution was allowed to warm to $23\text{ }^{\circ}\text{C}$ and stirred for 24 h. The resultant solution was quenched with water (15 mL) and the resultant mixture was extracted with dichloromethane (3 x 20 mL). The combined organic layers were washed with saturated aqueous sodium chloride solution (15 mL), dried over anhydrous sodium sulfate, and the dried solution was concentrated. The dried concentrate was purified by flash column chromatography (silica gel, 5% ethyl acetate–hexanes) to afford crude **3.25** (169 mg) as a yellow-black oil. Grubbs second-generation catalyst (24 mg, 0.028 mmol, 0.05 equiv) was added in one portion to **3.25** (169 mg) in dichloromethane (10.3 mL) at $23\text{ }^{\circ}\text{C}$. The resultant red solution was heated at $65\text{ }^{\circ}\text{C}$ for 48 h, then cooled to $23\text{ }^{\circ}\text{C}$ and concentrated. The resultant black residue was purified by flash column chromatography (silica gel, 5% ethyl acetate–hexanes) to afford **3.26** (80 mg, 0.30 mmol, 31% over 2 steps) as a white solid.

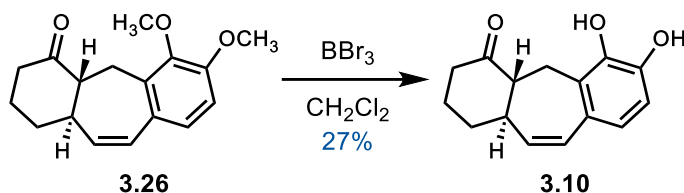
^1H NMR (400 MHz, CDCl_3) δ : 6.88 (d, $J = 8.4$ Hz, 1H), 6.71 (d, $J = 8.4$ Hz, 1H), 6.34 (dd, $J_1 = 12.4$, $J_2 = 2.4$ Hz, 1H),

5.59 (dd, $J_1 = 12.4$, $J_2 = 3.1$ Hz, 1H), 4.20 (dd, $J_1 = 15.1$, $J_2 = 1.0$ Hz, 1H), 3.85 (s, 3H), 3.75 (s, 3H), 2.56 (tq, $J_1 = 12.0$, $J_2 = 2.9$ Hz, 1H), 2.49 – 2.41 (m, 2H), 2.33 – 2.19 (m, 2H), 2.12 (ddq, $J_1 = 12.5$, $J_2 = 6.0$, $J_3 = 3.0$ Hz, 1H), 2.07 – 2.00 (m, 1H), 1.75 (qt, $J_1 = 13.2$, $J_2 = 4.1$ Hz, 1H), 1.63 – 1.57 (m, 1H).

^{13}C NMR (101 MHz, CDCl_3) δ :

211.1, 132.6, 129.0, 127.2, 110.0, 77.8, 77.5, 77.2, 56.2, 54.9, 50.8, 41.6, 33.53, 26.8, 24.4.

Synthesis of Analog 3.10



Boron tribromide (1.0 M in dichloromethane, 0.81 mL, 0.81 mmol, 2.75 equiv) was added dropwise to a solution of **3.26** (80 mg, 0.30 mmol, 1.0 equiv) in dichloromethane (1.9 mL) cooled at -40°C . The reaction mixture was stirred for 3 h and then quenched with water (5 mL) and the resultant mixture was extracted with dichloromethane (3 x 10 mL). The combined organic layers were washed with saturated aqueous sodium chloride solution (10 mL) and dried over anhydrous sodium sulfate. The dried solution was then concentrated. The resultant residue was first purified by flash column chromatography (silica gel, 20% ethyl acetate–hexanes) and then purified by high-pressure liquid chromatography to afford **3.10** (19.8 mg, 0.081 mmol, 27%) as a white solid.

^1H NMR (600 MHz, CDCl_3) δ : 7.93 (s, 1H), 6.78 (d, $J = 8.2$ Hz, 1H), 6.62 (d, $J = 8.1$ Hz, 1H), 6.56 (dd, $J_1 = 10.1, J_2 = 1.9$ Hz, 1H), 5.84 (dd, $J_1 = 10.1, J_2 = 5.6$ Hz, 2H), 3.19 (ddt, $J_1 = 13.2, J_2 = 7.1, J_3 = 1.2$ Hz, 1H), 3.05 (d, $J = 14.0$ Hz, 1H), 2.49 – 2.36 (m, 3H), 2.15 – 2.08 (m, 1H), 2.04 – 1.91 (m, 2H), 1.82 (qd, $J_1 = 12.7, J_2 = 4.1$ Hz, 1H), 1.66 – 1.57 (m, 1H), 0.90 – 0.81 (m, 2H).

^{13}C NMR (151 MHz, CDCl_3) δ : 216.4, 145.2, 141.4, 132.5, 131.3, 131.3, 126.3, 121.0, 112.7, 65.7, 44.9, 40.9, 30.5, 26.9, 24.6.

TLC:

20% ethyl acetate–hexanes, $R_f = 0.17$

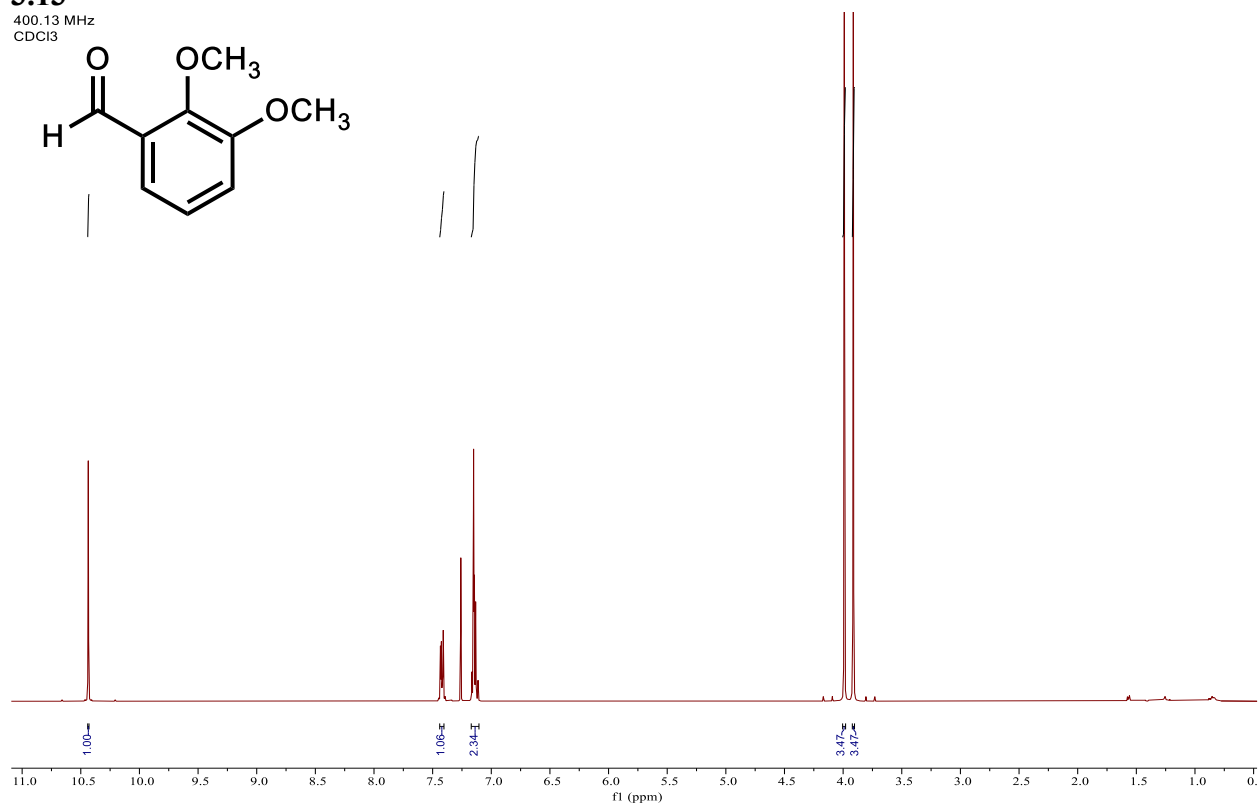
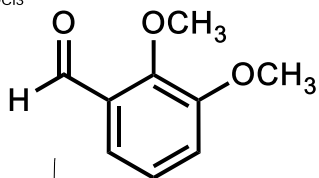
(UV, FeCl_3).

Appendix

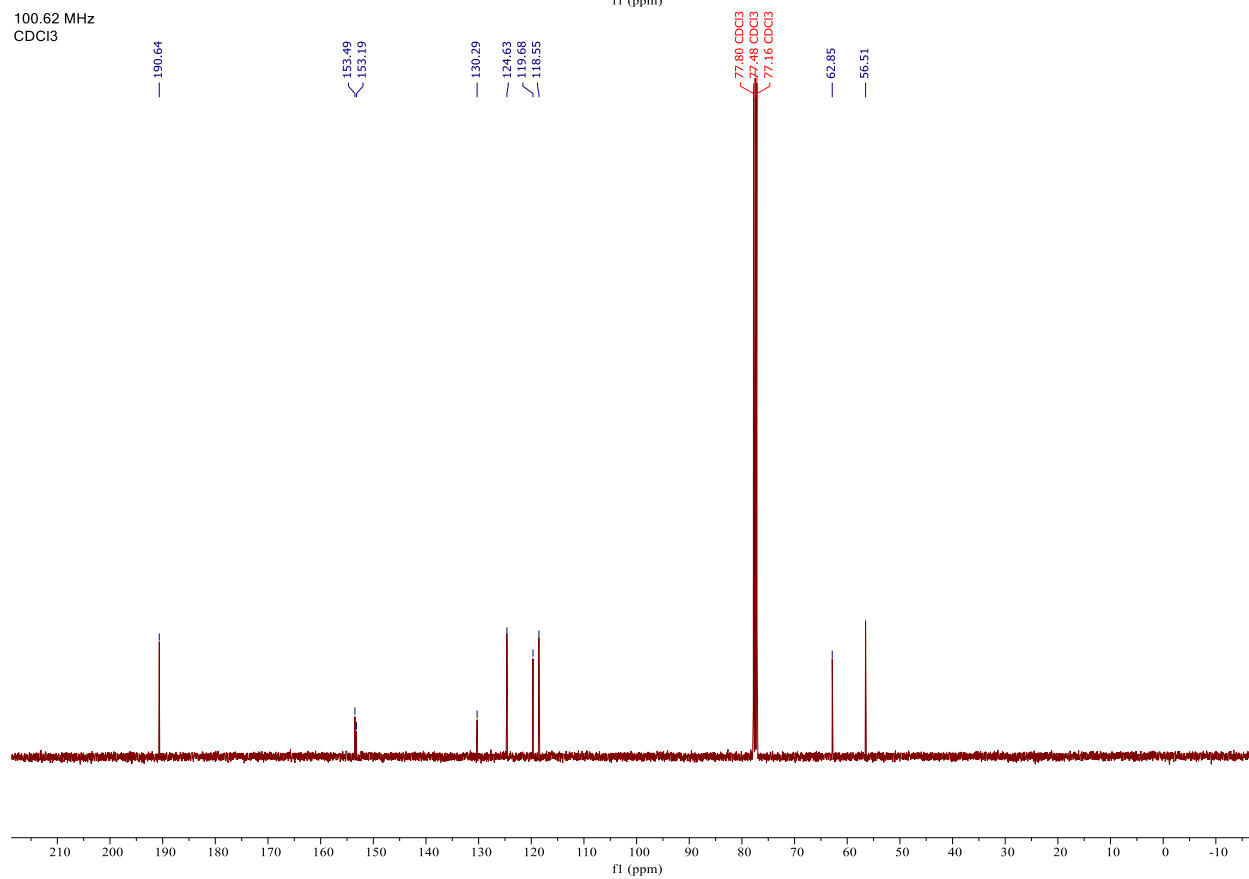
A. Catalog of Spectra

3.13

400.13 MHz
CDCl₃

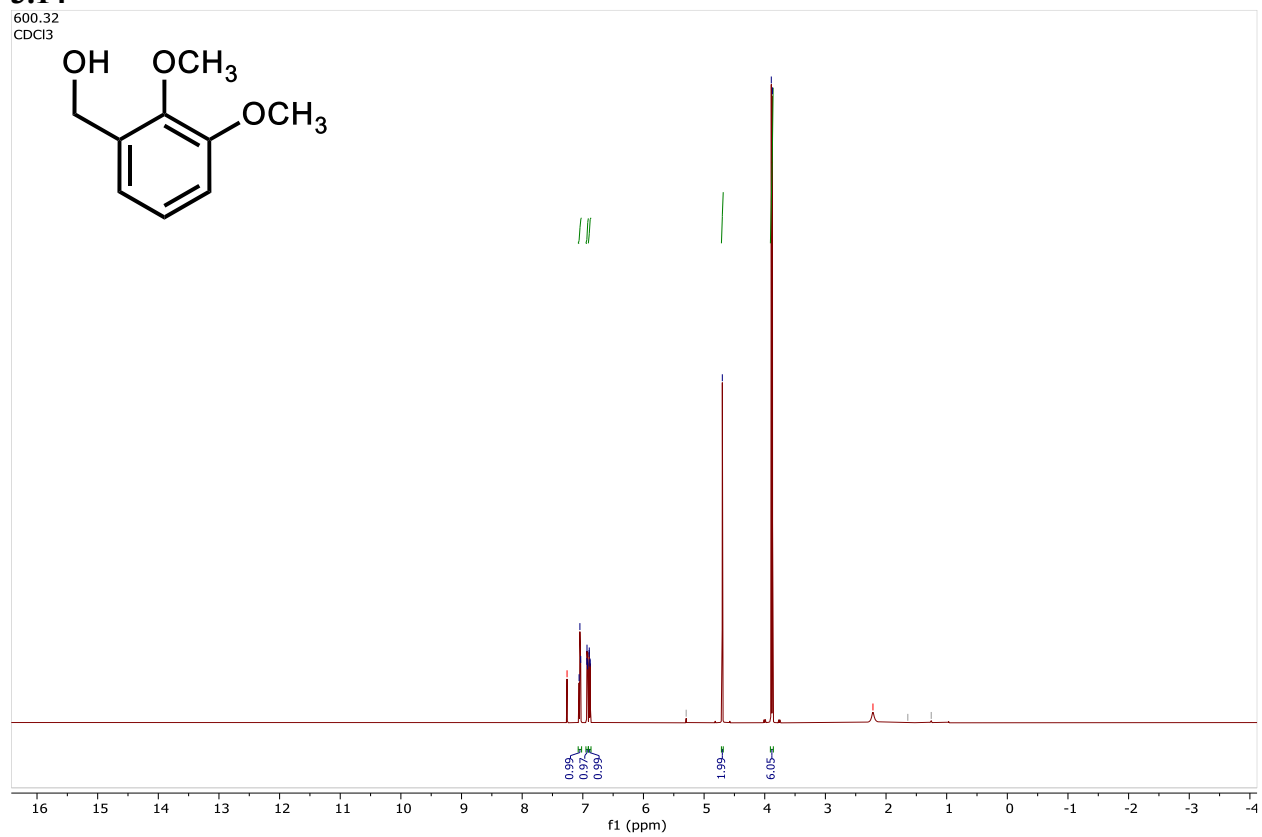
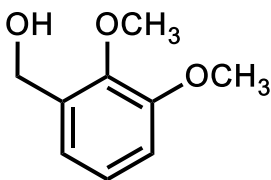


100.62 MHz
CDCl₃

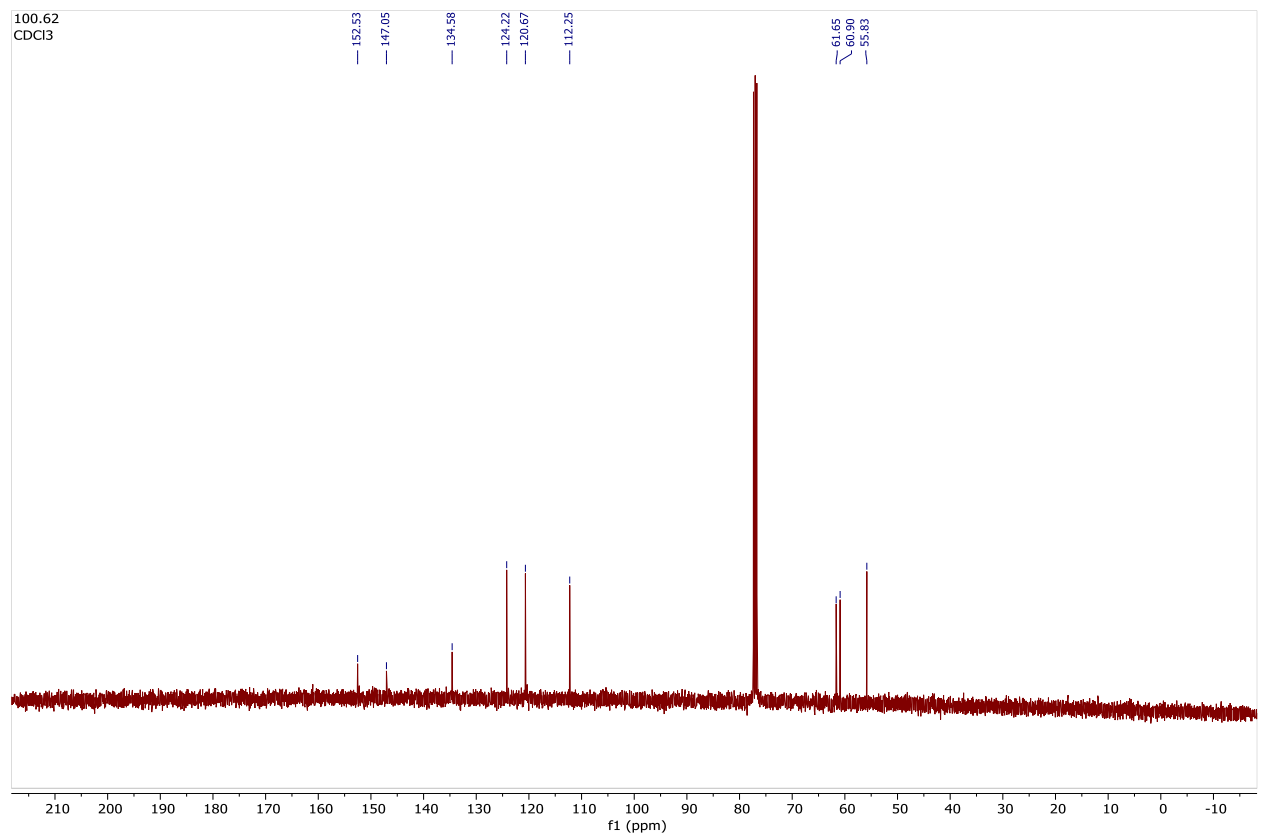


3.14

600.32
CDCl₃

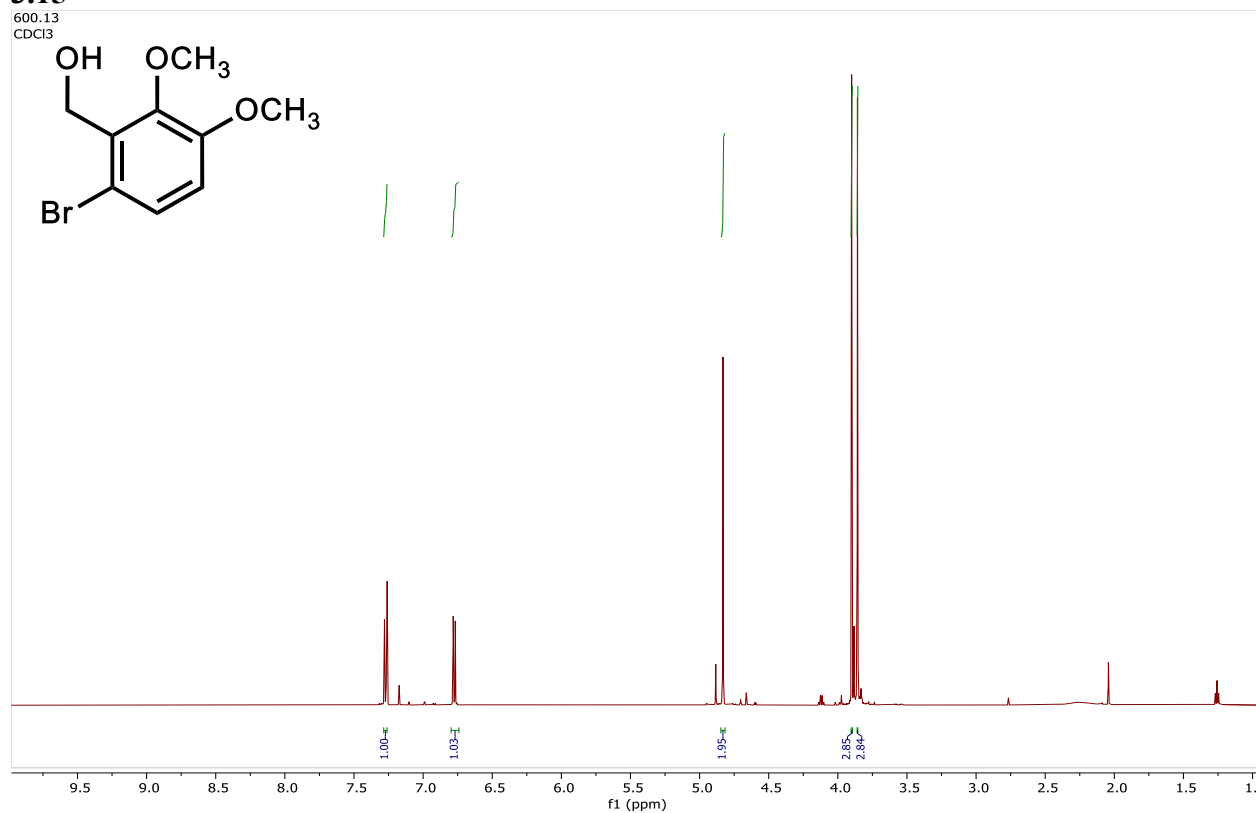
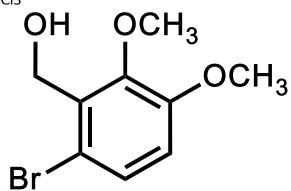


100.62
CDCl₃

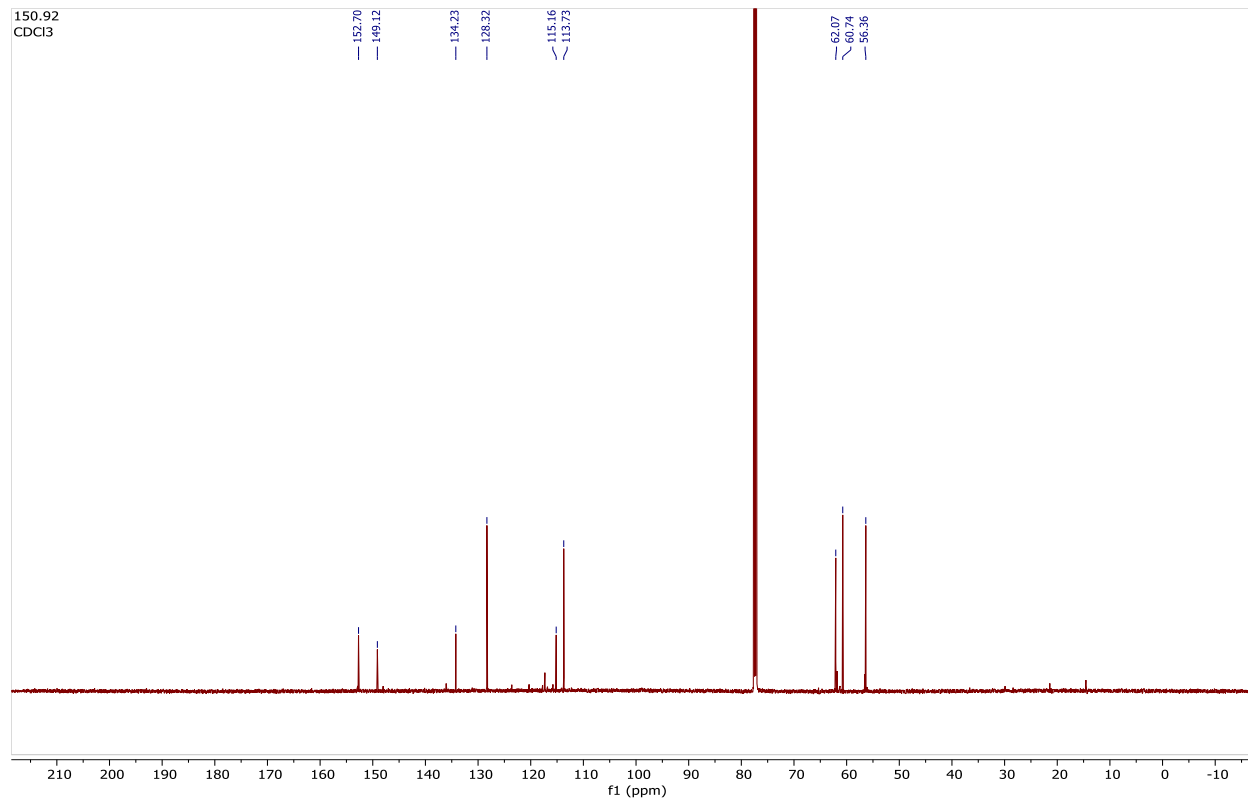


3.15

600.13
CDCl₃

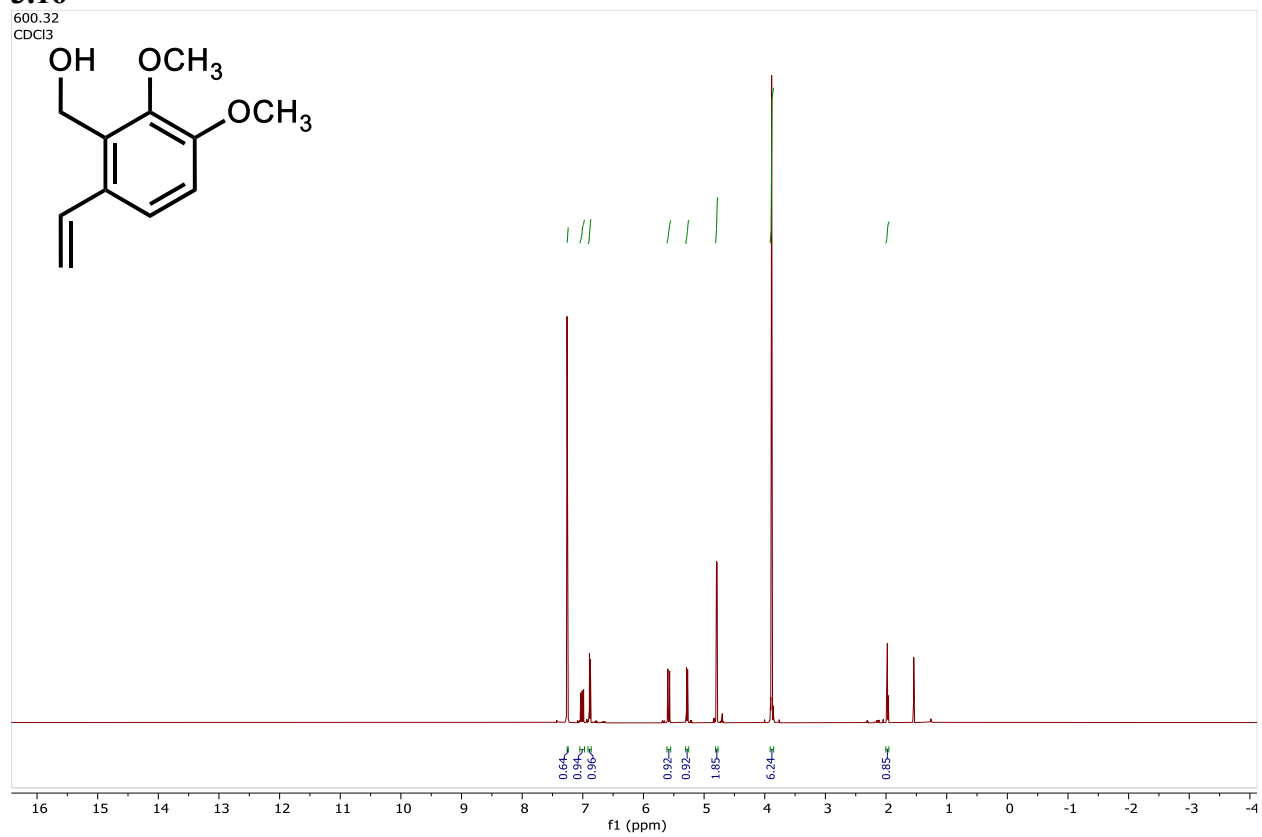
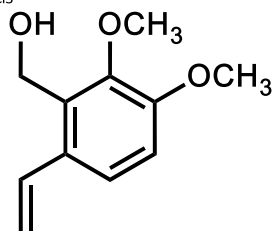


150.92
CDCl₃

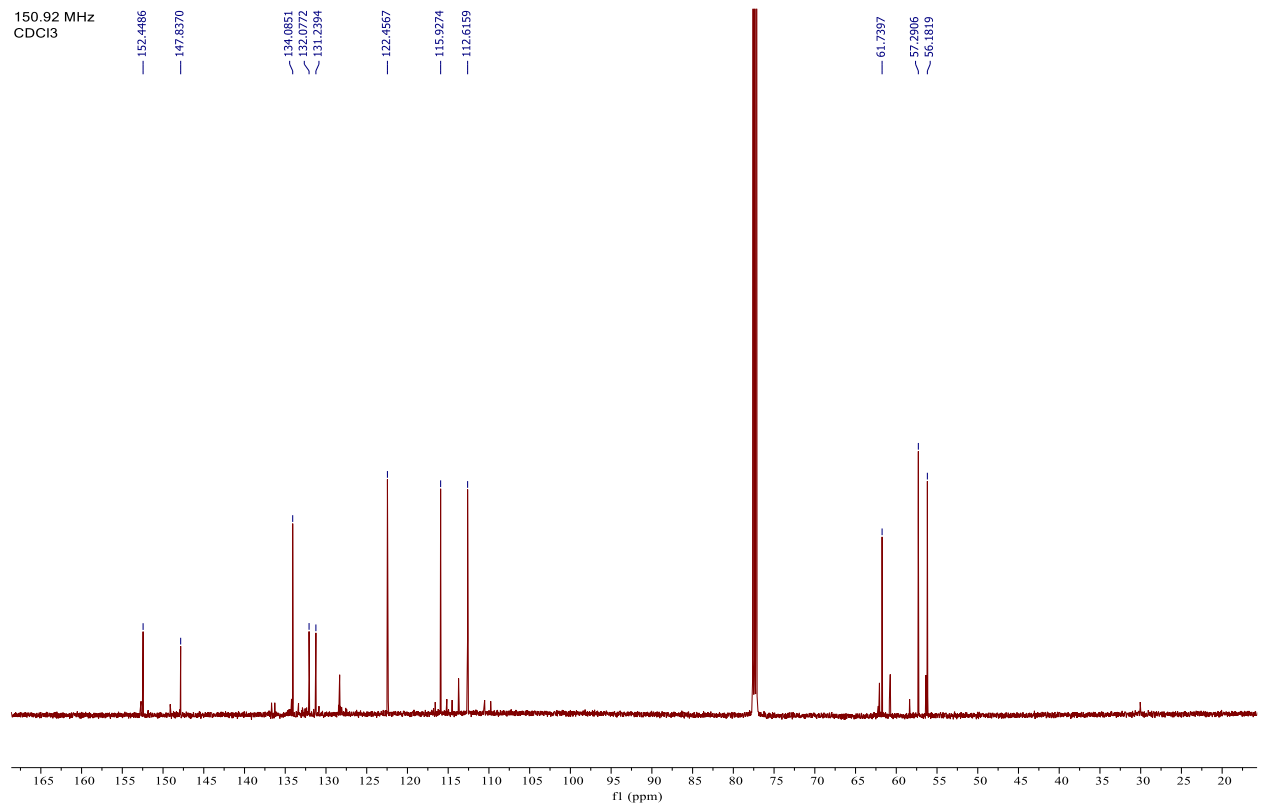


3.16

600.32
CDCl₃

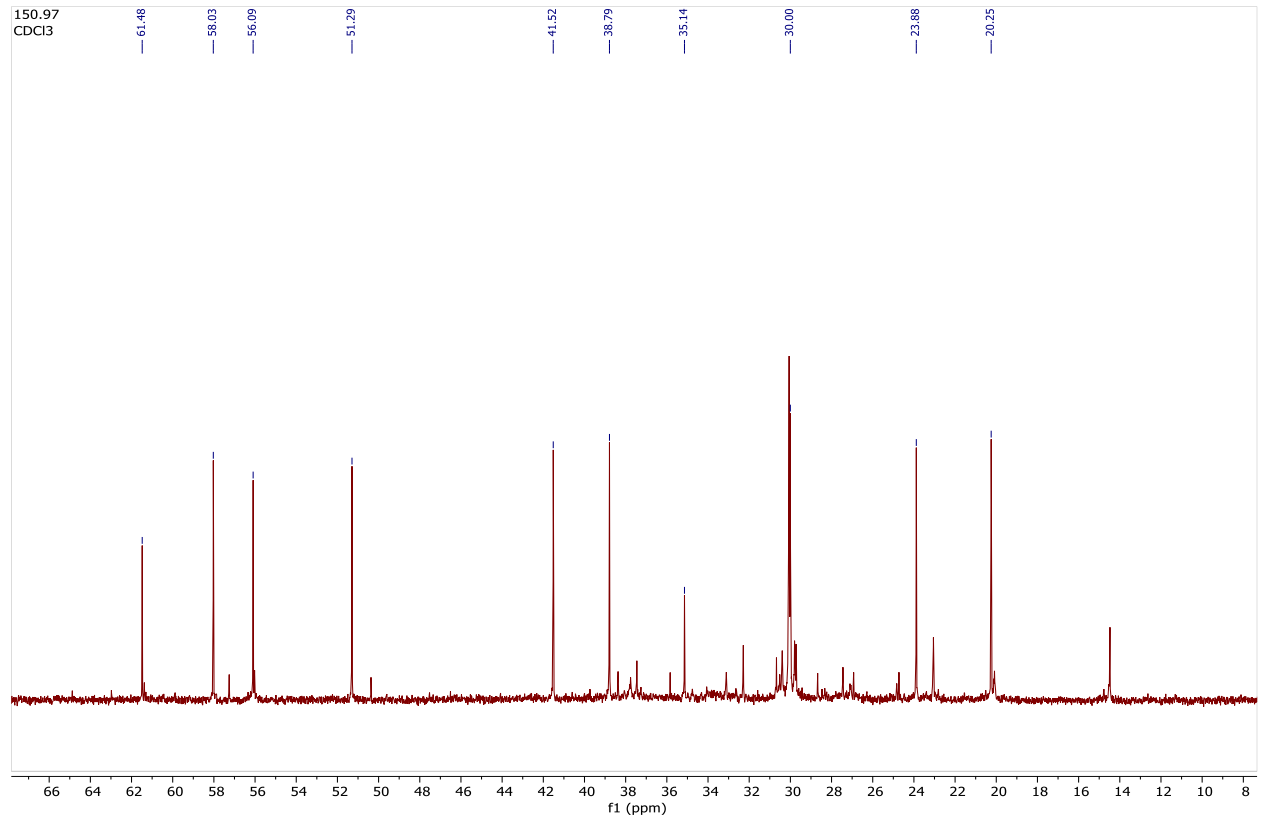
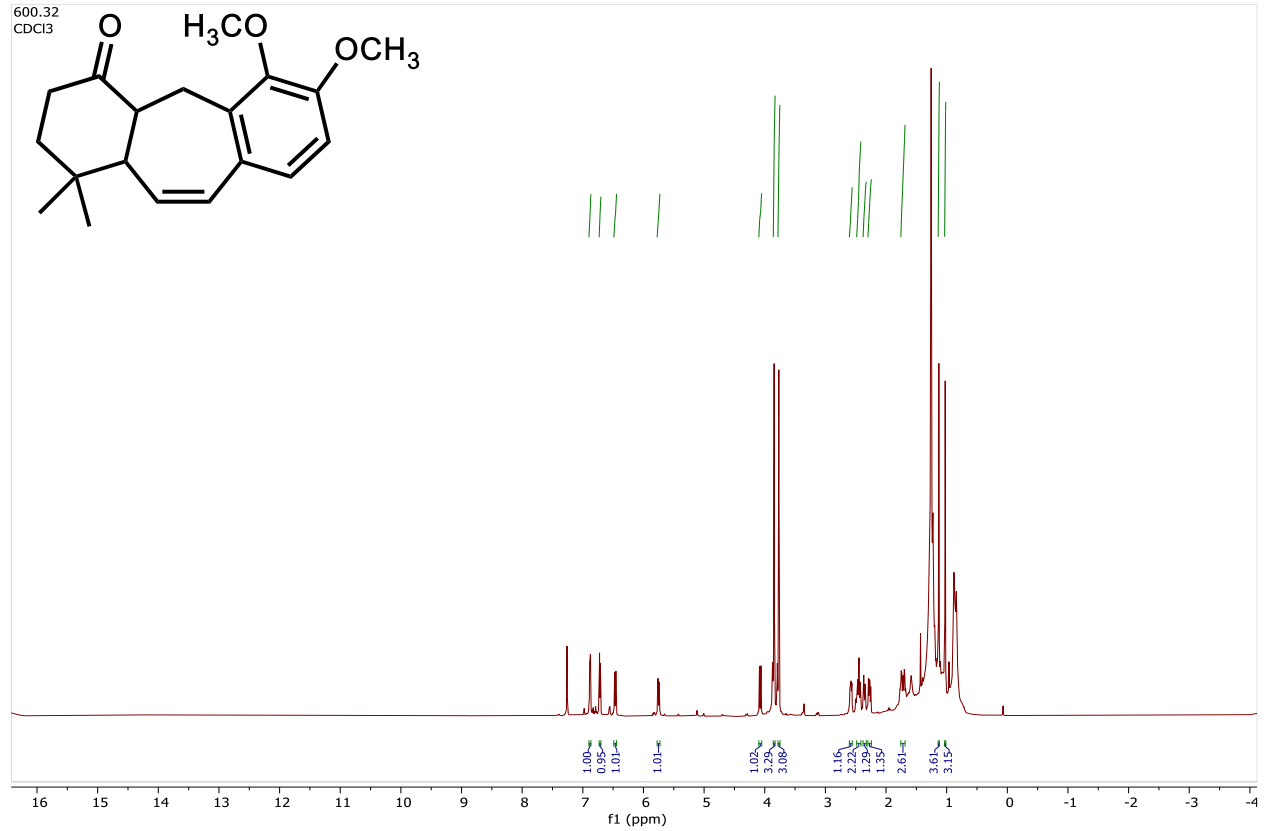


150.92 MHz
CDCl₃



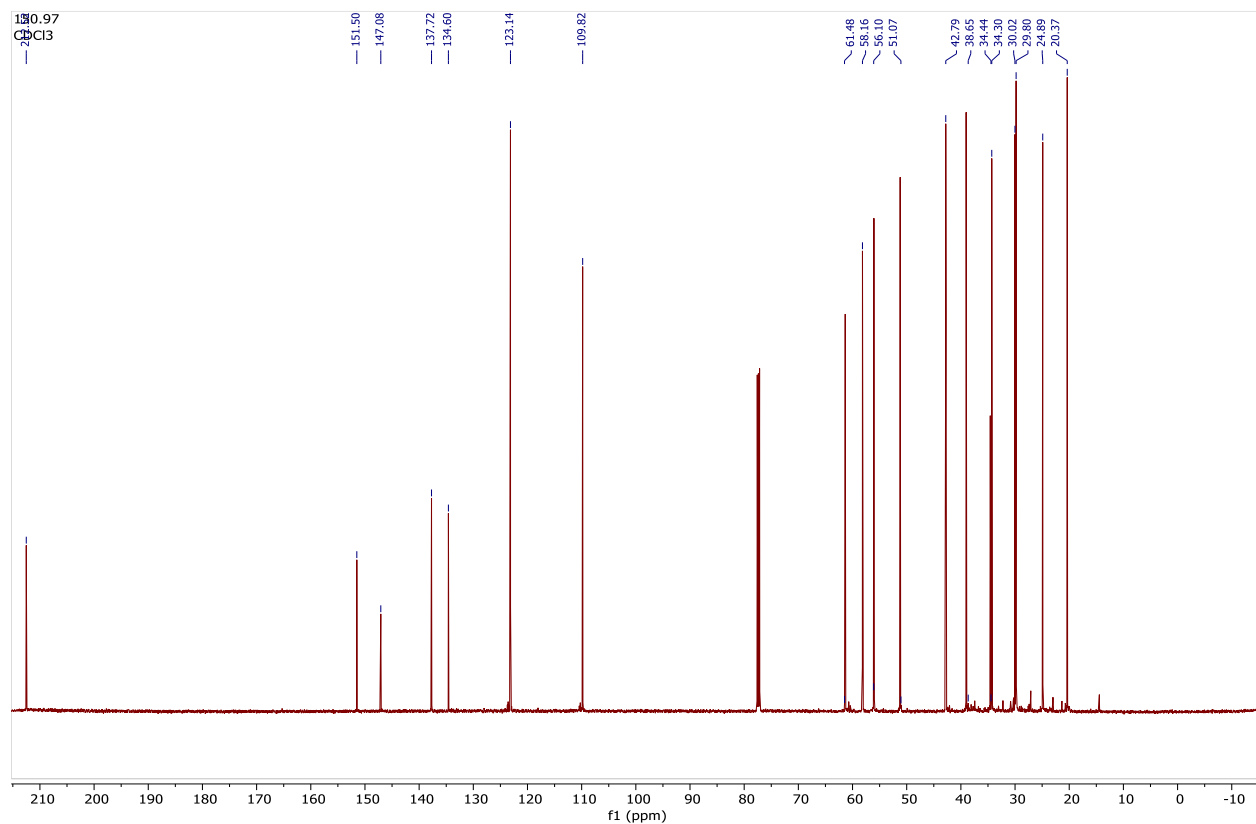
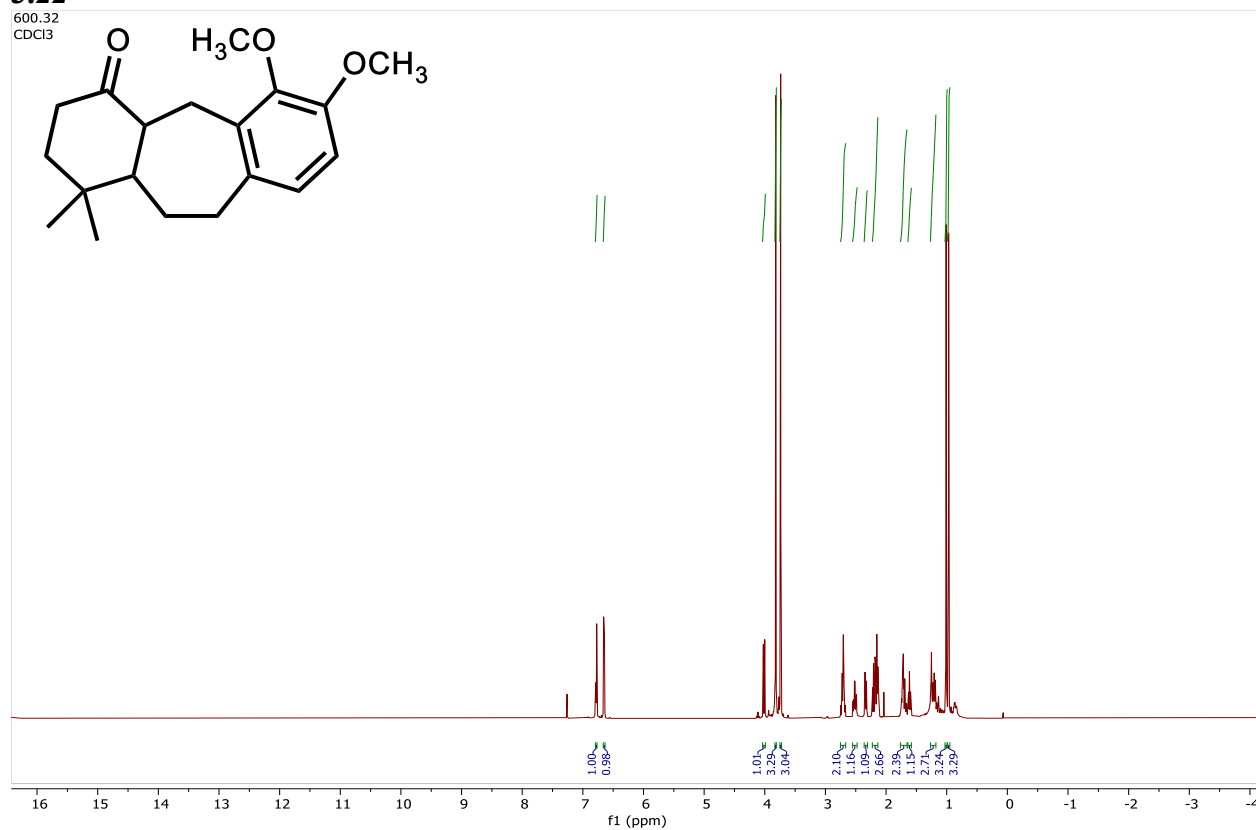
3.21

600.32
CDCl₃



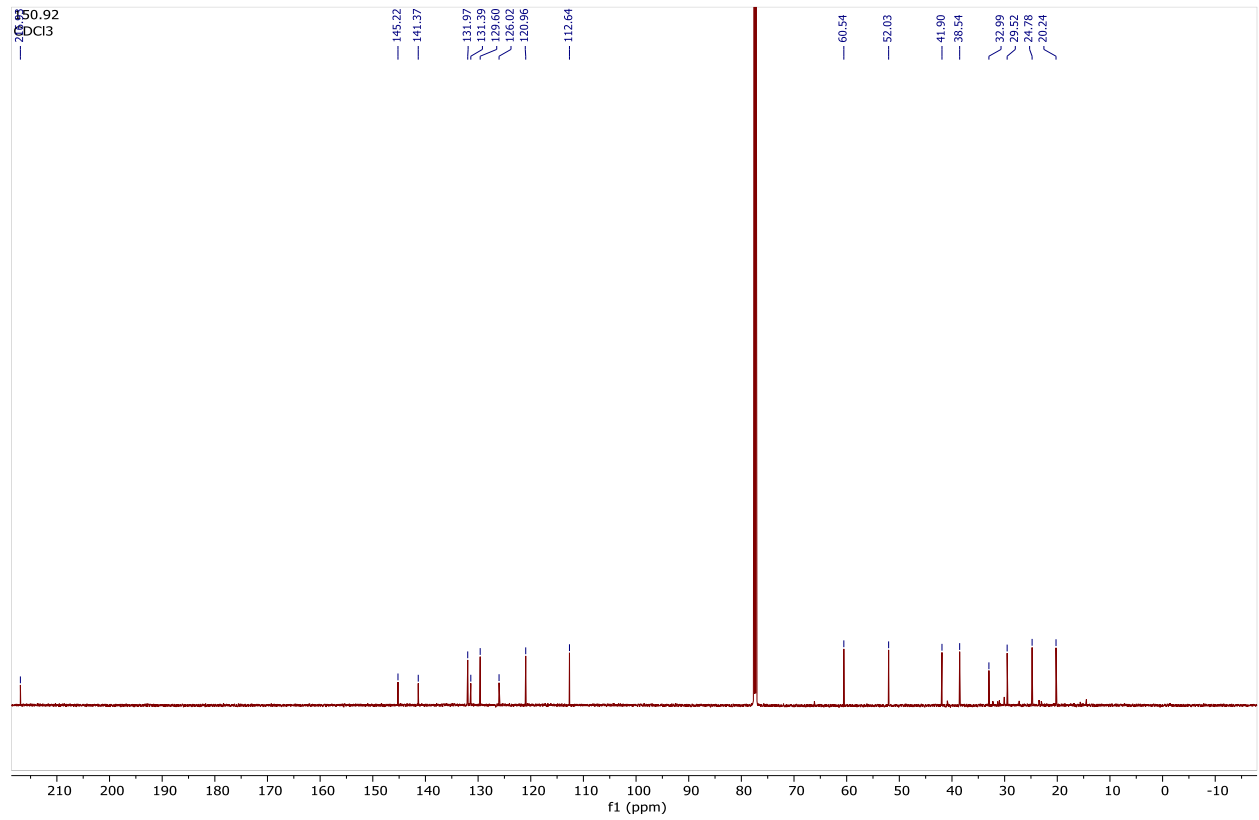
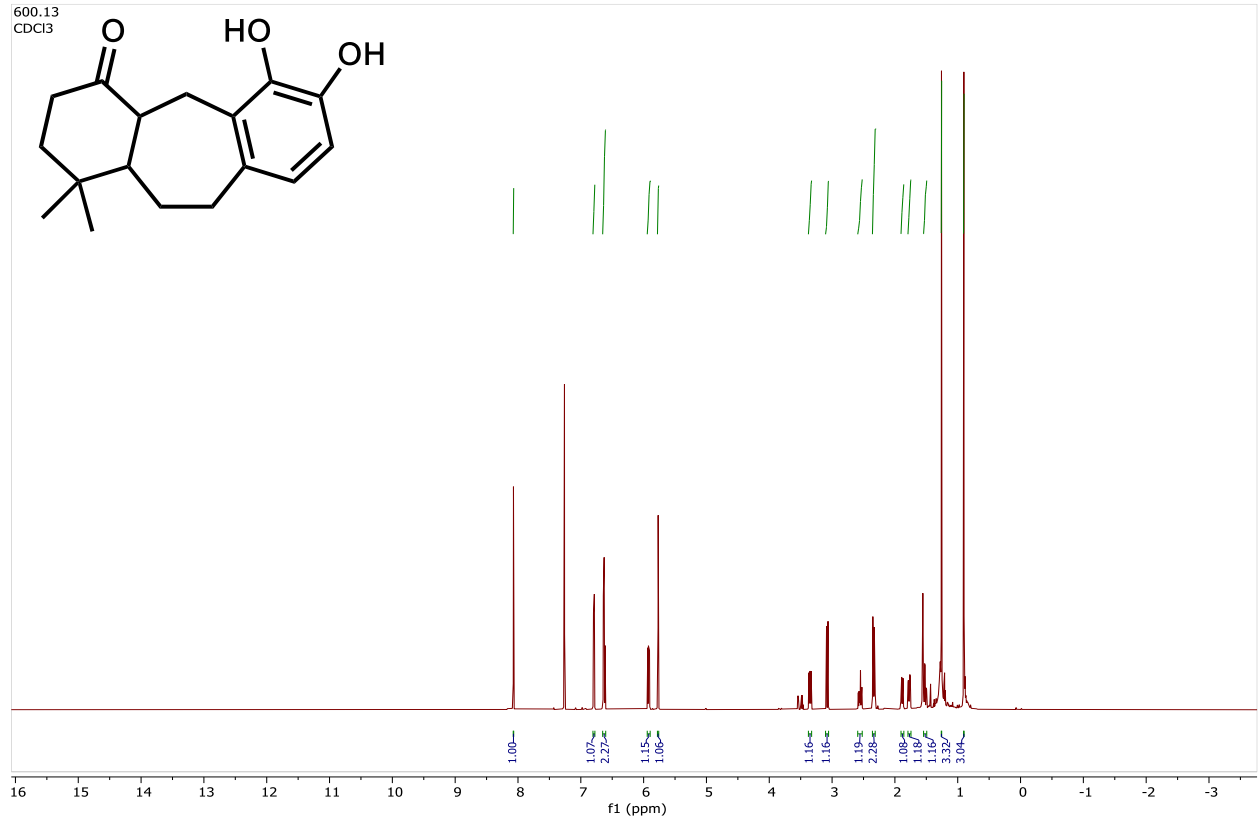
3.22

600.32
CDCl₃



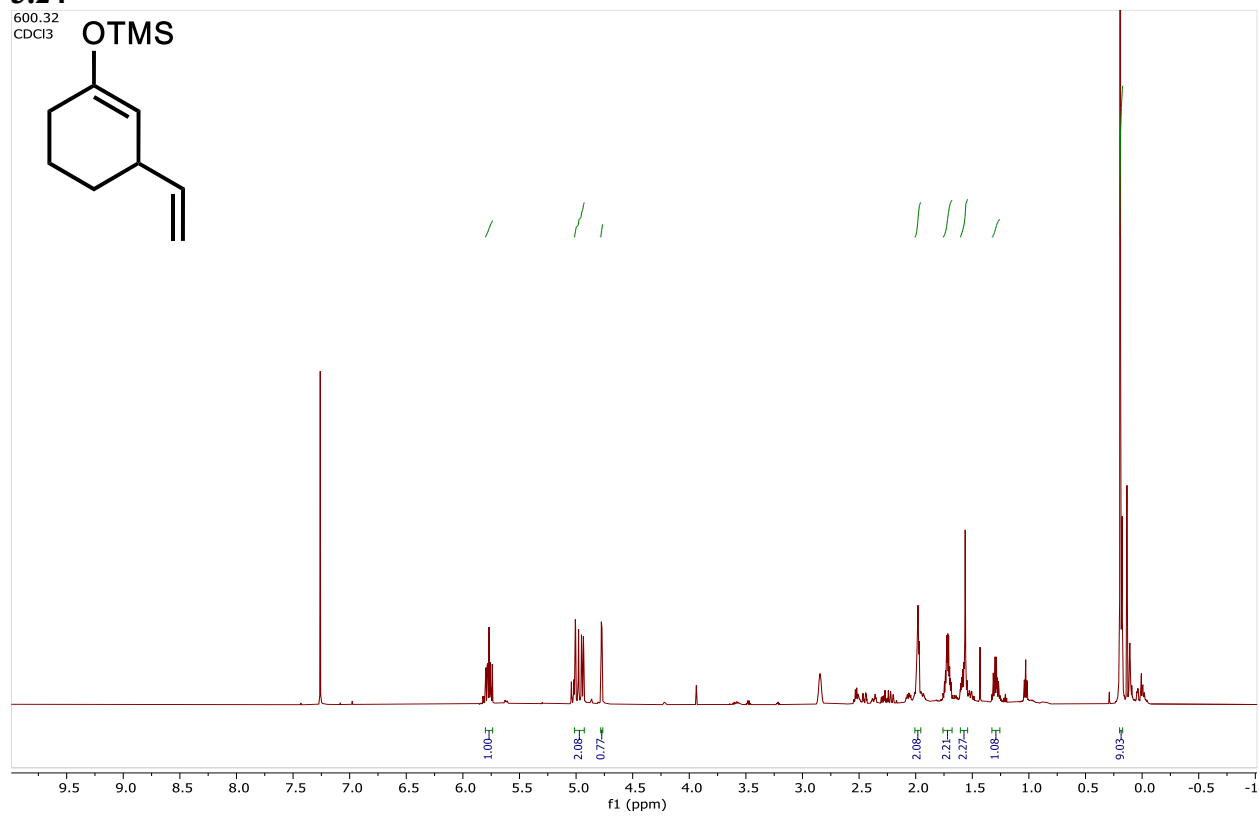
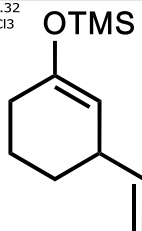
3.9

600.13
CDCl₃

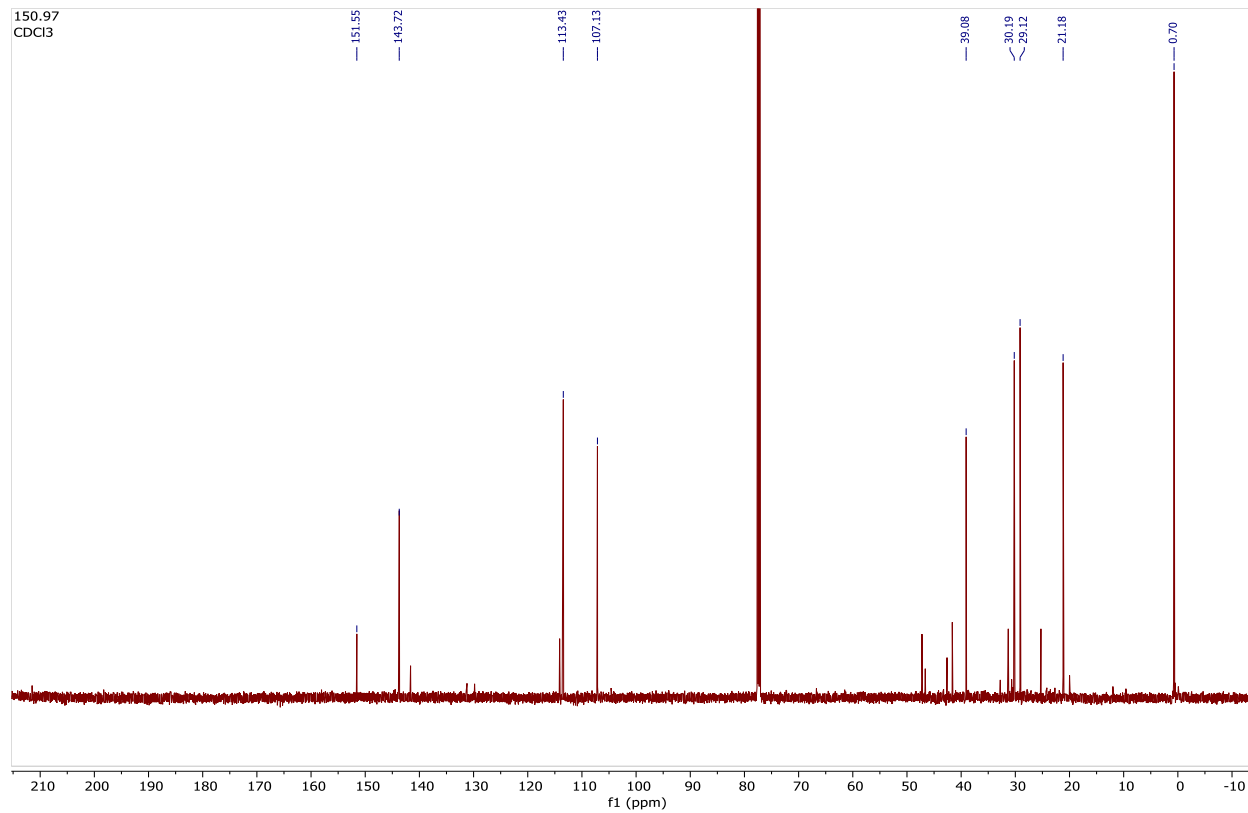


3.24

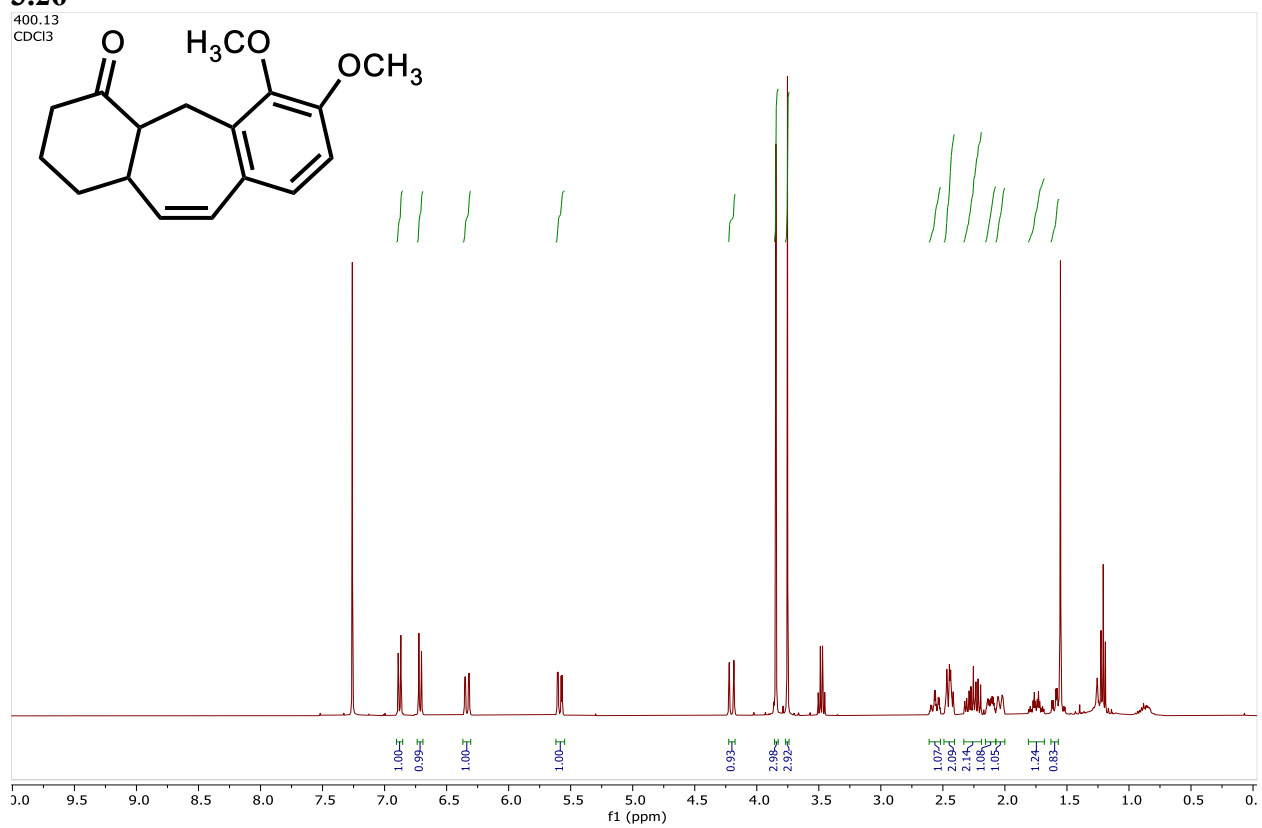
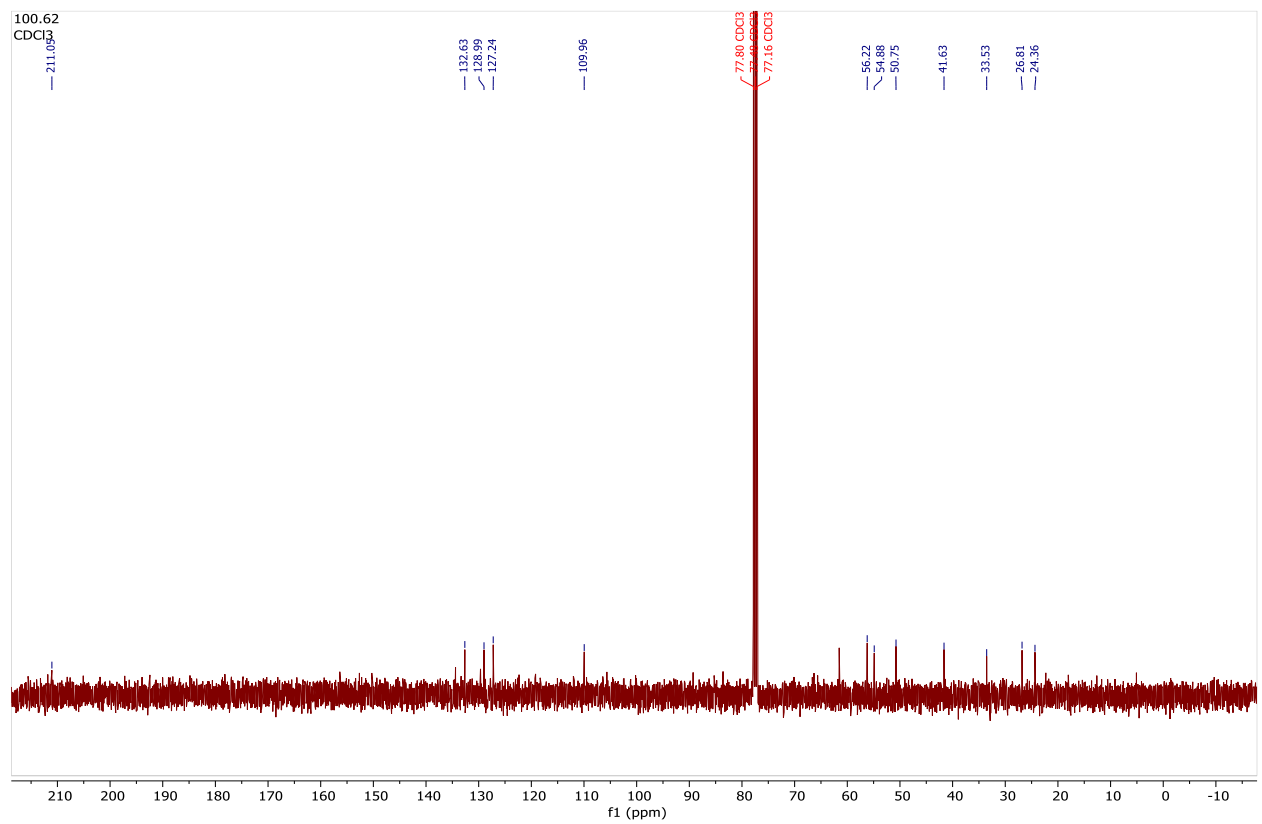
600.32
CDCl₃



150.97
CDCl₃

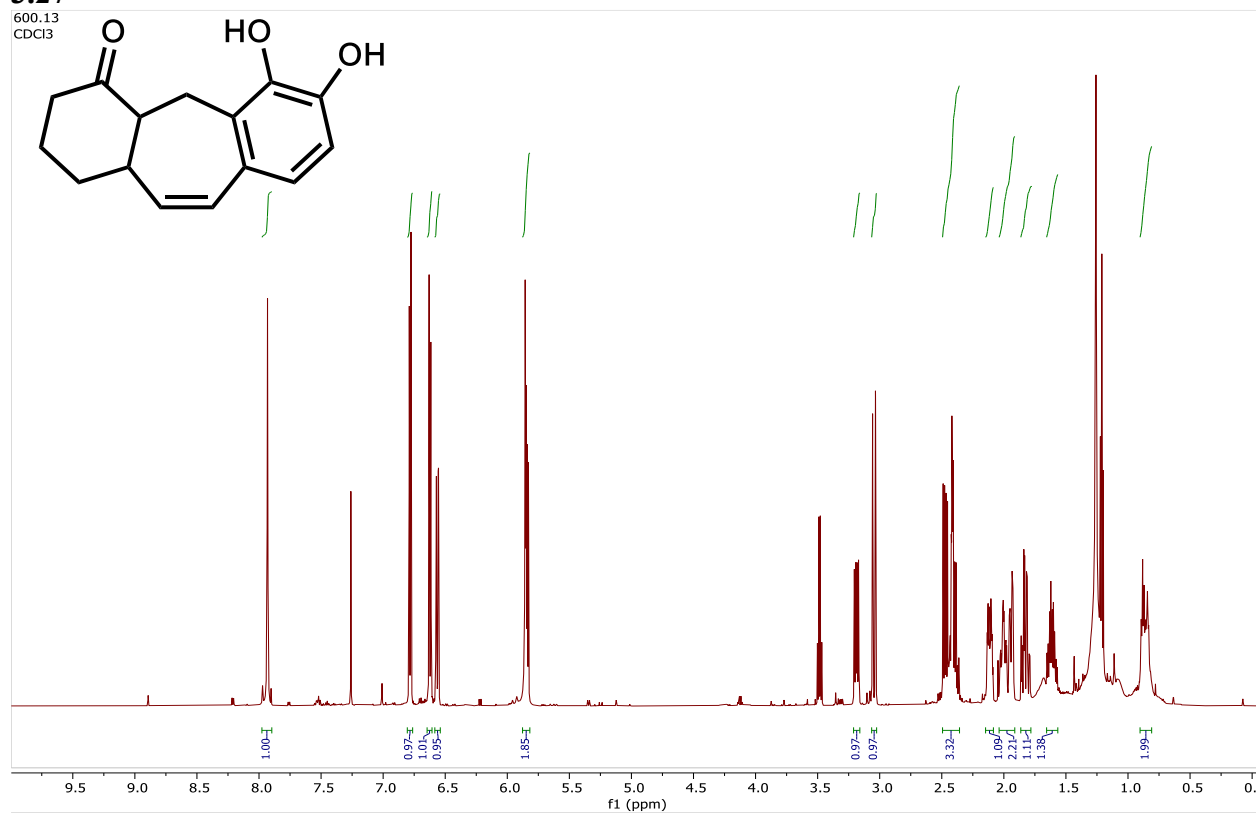
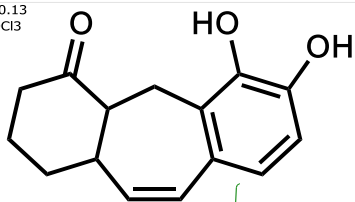


3.26

400.13
CDCl₃100.62
CDCl₃

3.27

600.13
CDCl3



50.92
CDCl3

